TECHNICAL REPORT Report No.: ESSO-INCOIS-OMARS-TR-06(2024)

Evaluation of INCOIS operational general circulation ocean model forecasted fields

By

Hasibur Rahaman, U Srinivasu and T M Balakrishna Nair

Indian National Centre for Ocean Information Services (INCOIS),Earth System Science Organization (ESSO), Ministry of Earth Sciences (MoES), Hyderabad, India

www.incois.gov.in

May, 2024

DOCUMENT CONTROL SHEET
Earth System Science Organization (ESSO)
Ministry of Earth Sciences (MoES)
Indian National Centre for Ocean Information Services (INCOIS)

ESSO Document Number: ESSO-INCOIS -OMARS-TR-06(2024)

Title of the report: Evaluation of INCOIS operational general circulation ocean model forecasted fields

Author(s):

[Rahaman Hasibur, Srinivasu U and Nair Balakrishna TM]

Originating unit: OMARS

Type of Document: Technical Report (TR)
Number of pages:52
Number of figures: 42
Number of references: 36
Keywords: Ocean model, Ocean forecast, ROMS, HYCOM, Validation
Security classification: Open
Distribution: Open
Date of publication: May 2024

Abstract (250 words):
INCOIS is mandated to provide the forecast of the ocean state for the Indian Ocean as well as the associated neighboring Regional Integrated Multi-Hazard Early Warning System (RIMES) countries. Apart from the common public associated maritime industries, the Indian Coast Guard, Shipping Corporation of India, and Oil and Natural Gas Corporation (ONGC) also use INCOIS forecasted products. The forecast is given to users starting from fishermen to the Indian Navy and Coast Guard. The 7-day forecast is generated daily and given to the users operationally every day. These parameters are generated by running two models ROMS and HYCOM. In this report, we validated the sea surface temperature (SST), surface and sub-surface currents, mixed layer depth (MLD), and thermocline depth (represented as 20 deg isotherm: D20) first-day forecast generated by the general circulation models with observations from moored buoys, satellite observations, and analysis. We also used acoustic doppler current profiler (ADCP) current observations to evaluate the sub-surface current forecast. Although there are significant differences in the configurations, however, both models are shown to be statistically equivalent with consistent spatial and temporal patterns indicating the main differences are attributable to unrepresented processes. Overall ROMS performance is slightly better than HYCOM in SST. For the current HYCOM performance is superior to ROMS. The enhanced resolution in ROMS from 1/12 degrees to 1/48 degrees, degrades both the current and SST forecast. HYCOM performance is much better for the first day MLD and D20 forecast as compared to ROMS. For MLD and D20 forecast ROMS1/12 performs better than ROMS1/48.

Table of Content

Evaluation of INCOIS operational general circulation ocean model forecasted fields

Rahaman Hasibur, Srinivasu U and Nair Balakrishna TM

Abstract

INCOIS is mandated to provide the forecast of the ocean state for the Indian Ocean as well as the associated neighboring Regional Integrated Multi-Hazard Early Warning System (RIMES) countries. Apart from the common public associated maritime industries, the Indian Coast Guard, Shipping Corporation of India, and Oil and Natural Gas Corporation (ONGC) also use INCOIS forecasted products. The forecast is given to users starting from fishermen to the Indian Navy and Coast Guard. The 7-day forecast is generated daily and given to the users operationally every day. These parameters are generated by running two models ROMS and HYCOM. In this report, we validated the sea surface temperature (SST), surface and sub-surface currents, mixed layer depth (MLD), and thermocline depth (represented as 20 deg isotherm: D20) first-day forecast generated by the general circulation models with observations from moored buoys, satellite observations, and analysis. We also used acoustic doppler current profiler (ADCP) current observations to evaluate the sub-surface current forecast. Although there are significant differences in the configurations, however, both models are shown to be statistically equivalent with consistent spatial and temporal patterns indicating the main differences are attributable to unrepresented processes. Overall ROMS performance is slightly better than HYCOM in SST. For the current HYCOM performance is superior to ROMS. The enhanced resolution in ROMS from 1/12 degrees to 1/48 degrees, degrades both the current and SST forecast. HYCOM performance is much better for the first day MLD and D20 forecast as compared to ROMS. For MLD and D20 forecast ROMS1/12 performs better than ROMS1/48.

1. Introduction

India has a long coastline extending well over 7500 km and an Exclusive Economic Zone (EEZ) covering about 2.3 million sq. km. About one-fourth of the country's population lives in the coastal regions. A large fraction of this population directly or indirectly depends on the surrounding ocean for a wide spectrum of activities and resources, such as traditional fishing, high-tech offshore industries, ports and harbors, shipping, and tourism. Maritime security and safety at sea and shipping, monitoring of oil spills and pollutants for the protection of the marine environment as well as offshore commercial operations demand accurate information and predictions of the state of the ocean in different spatial and temporal scales. Accurate prediction of ocean currents is important for maritime safety, hazardous chemical spills, fisheries, the oil and gas industry, and national security. Information on currents is used for search and rescue, tracking of oil spills, safe navigation, shipping, and naval operations, design of port and coastal infrastructure, and safe recreational activities (Saima et al. 2023). Although the verification of ocean variables such as temperature, salinity, and sea level in ocean forecast systems is routinely undertaken as part of the operational ocean forecast systems, the verification of ocean currents is less common in part due to the challenges of real-time quality control and because of the scarcity of ocean current data. Satellite-tracked drogued drifting buoys can travel several thousand kilometers and provide global geographic coverage, and ocean currents observed from these drifters have been used to verify global ocean forecast systems (Blockley et al., 2012). However, difficulties exist to validate against these global drifters, where unresolved, or unmodelled inertial currents and tides, along with the Lagrangian effects such as Stokes drift must be accounted for. Also, coastal currents are not well observed by drifters. Recently Saima et al. (2023) have evaluated the surface current forecasts from 4 global operational centres Australian Bureau of Meteorology (ABoM) for verification and inter-comparison with Mercator Océan International ocean forecast system (MOi), the operational models of the Met Office, UK: Forecast Ocean Assimilation Model (FOAM) and Coupled Atmosphere-Land-Ocean-Ice Data Assimilation (CPLDA) systems, and the Global Ice Ocean Prediction System (GDPS-GIOPS) at the Canadian Centre for Meteorological and Environmental Prediction (CCMEP) and showed Zonal currents have a stronger signal than the meridional currents as indicated by their high correlation with observations, and lower errors. This indicates zonal currents on average are more predictable and persistent than the meridional currents, resulting in improved representation in the models. Hyder et al (2012) evaluated hindcasted Surface currents for 2007–2008 from the Forecast Ocean Assimilation Model (FOAM) Global and Indian Ocean models against observations from 46 global tropical moored buoys over the Indian Ocean. They also reported similar results to that of Saima et al. (2023) that Zonal (u) currents are less challenging to model than meridional flows (v). The assimilative global model has a reasonable skill for zonal currents but less skill for meridional currents. The assimilative models have higher skill than the corresponding non-assimilative models. A too-strong westward bias of the order of 20 cm/s is evident along the equator in all model versions used in Saima et al. (2023). No extra skill is evident in the high-resolution (1/12°) regional model compared to the coarser resolution (1/4°) global model.

INCOIS developed an operational ocean forecasting system to provide the forecast to the coastal people of India as well as the associated neighboring RIMES countries. The forecasts are given to users starting from fishermen to the Indian Navy and Coast Guard. Seven (7) day advance forecasts are generated daily and given to the users operationally every day. Forecasting systems are typically composed of three independent components, the numerical ocean circulation model, observations, and the data assimilation (DA) technique. Such systems incorporate information from observations in synergy with high-resolution ocean models to produce estimates of the ocean state better than what can be obtained by using either measurements or models in isolation. This report compares the simulated forecasted first-day surface and sub-surface currents sea surface temperature (SST), MLD, and D20 from two operational OGCMS i,e ROMS and HYCOM at INCOIS. These current data are independent since they are not assimilated by the models. However, the associated temperature and salinity observations at the same sets of moorings are assimilated.

2. Operational Ocean General Circulation Models (OGCMs) at INCOIS

2.1 Regional Ocean Modeling System (ROMS)

INCOIS started issuing basin-scale forecasts of a few oceanographic parameters such as SST, mixed layer depth, surface currents, and depth of the 20°C isotherm based on a relatively low-resolution (1/4°) Regional Ocean Modeling System (ROMS) configuration for the Indian Ocean in January 2010. The domain of the Indian Ocean model based on ROMS (i.e., O-ROMS) extends from 30°E to 120°E in the east-west direction and from 30°N to 30°S in the north-south direction. This forecast system named as "Indian Ocean Forecast System" (INDOFOS). The spatial resolution of INDOFOS was upgraded to 1/8° in March 2012 (Francis et al. 2013). This forecast was issued using stand-alone ROMS with every 6 hly atmospheric forcing from the atmospheric model GFS (Prasad et al. 2016) without any data assimilation schemes. Subsequently, the horizontal grid spacing of operational ROMS (O-ROMS) was upgraded to 1/12° for the Indian Ocean basin under the project named Indian Ocean High-Resolution Operational Ocean Forecast and Reanalysis System (HOOFS) and given the name IO-HOOFS. Further another high resolution 1/48 degree north Indian Ocean was also operationalized at the same time (Francis et al. 2021). Further under the "Ocean Modeling Data Assimilation and Process Specific Observations" (O-MASCOT) project a data assimilation system named Regional Analysis of Indian Ocean (RAIN) was developed. In the RAIN Local Ensemble Transform Kalman Filter (Hunt et al. 2007) data assimilation scheme was implemented in the operation 1/12 degree Regional Ocean Modeling System as the corrective measure to improve the quality of the ocean states (Baduru et al. 2019). This data assimilation system is an ensemble-based ocean data assimilation system (Baduru et al. 2019), in which ocean observations are assimilated to the HOOFS configuration using a localized ensemble transform Kalman filter (LETKF) assimilation scheme. LETKF is a relatively new assimilation scheme, which is effective and computationally inexpensive, compared to other ensemble-based Kalman filters (Anderson 2007; Wang and Bishop 2003; Ott et al. 2004) since the assimilation of observations occurs in the ensemble space (Hunt et al. 2007). For preparing the regional analysis, the IO-HOOFS is forced by 80-member-ensemble atmospheric forcing produced by NCMRWF using a Global Forecast System (GFS) with horizontal resolution of 12 km.

INCOIS started providing global ocean analysis based on the global ocean data assimilation system (GODAS) in 2013 which was originally developed by the National Centers for Environmental Prediction (NCEP). INCOIS-GODAS is based on the MOM4p0d ocean model and 3DVar data assimilation scheme which assimilates observed temperature and salinity profiles from all in-situ observations over the global ocean (Ravichandran et al. 2013). GODAS subsequently upgraded with MOM4p1 which provides improved ocean analysis/reanalysis as compared to present operational INCOIS-GODAS (Rahaman et al. 2016;2018). In addition to providing the lateral boundary conditions for IO-HOOFS, INCOIS-GODAS also provides the oceanic initial conditions for the seasonal prediction of Indian monsoon using the Climate Forecast System, version 2 (CFSv2; Rao et al. 2019). Six-hourly atmospheric fields, obtained from the National Centre for Medium-Range Weather Forecast (NCMRWF), derived from the NCMRWF Unified Model (NCUM) at a horizontal resolution of ~25 km, are used to force the ocean state in O-ROMS and INCOIS-GODAS (George et al., 2016). Forecasted atmospheric fields from the NCMRWF Unified Model (NCUM) configured at a horizontal resolution of 12 km are used for forcing both NIO-HOOFS and IO-HOOFS setups in the forecast mode (Sumit Kumar et al. 2018).

2.2 HYbrid Coordinate Ocean Model (HYCOM)

Apart from ROMS-based forecast a state-of-the-art operational forecasting system based Hybrid Coordinate Model (HYCOM), with data assimilation (DA) is operational at INCOIS since March 2017. The Indian Ocean model is the highest resolution operational system with DA available for the basin compared to any operational agency in the world. The core of the system is a 1/16 degree eddy-resolving Indian Ocean Hybrid Coordinate Model (HYCOM), nested to a 1/4 Global HYCOM which provides lateral boundary conditions to the high-resolution model. The system uses a data assimilation scheme based on the Tendral Statistical Interpolation (T-SIS) scheme (Joseph et al. (2018).

We used the 2020 first-day forecast from IO-HOOFS (ROMS 1/12), NIO-HOOFS (ROMS 1/48), and HYCOM for the evaluation of SST, surface, and sub-surface current. However, for MLD and D20 we used 2023 first-day forecasts.

3. Forecast verification *What makes a forecast "good"?*

Allan Murphy, a pioneer in the field of forecast verification, wrote an essay on what makes a forecast "good"
(Murphy,1993). He distinguished three types of "goodness":

Consistency - the degree to which the forecast corresponds to the forecaster's best judgment about the situation, based upon his/her knowledge base
Quality - the degree to which the forecast corresponds to what actually happened
Value - the degree to which the forecast helps the a decision maker to realize some incremental economic and/or other benefit.

Forecast quality is not the same as forecast value. A forecast has high *quality* if it predicts the observed conditions well according to some objective or subjective criteria. It has *value* if it helps the user to make a better decision alternately one can ask *what is the relative improvement of the forecast over some reference forecast.* So for any parameter if robust climatology exists and if the forecast is better than this climatology, it has some value. Implies information about the value or worth of a forecast relative to an alternative (reference) forecast. In meteorology, the reference forecast is usually persistence (no change from most recent observation) or climatology. The *skill score* can be unstable for small sample sizes. This aspect can be quantified by computing skill score. A skill *score* measures the *accuracy* of a forecast with reference to the accuracy of a *standard forecast*. The standard forecast is usually but not always a forecast that is available to a forecaster, and which does not require any effort or knowledge on his part to prepare. For example, a forecast which consists of the climatological average temperature for a particular station for each day can be obtained from climatological tables and doesn't require any knowledge of the current weather situation to prepare.
A skill score is a comparison of the score obtained by a forecast with the score obtained by the standard forecast using the same set of verification data. The format of skill scores is usually the same and given as

$$\text{Skill Score} = \frac{\text{score for the forecast} - \text{score for the standard forecast}}{\text{perfect score} - \text{score for the standard forecast}} \qquad \text{Eqn ----(1)}$$

Forecast accuracy using skill score using Morphy's 1993 formula

Skill Score = 1 – (RMSD forecast/RMSD reference) Equ …..(2)

2 types of skill scores:
Persistence skill score with persistence as a reference
Climatology skill score with climatology as a reference

The lower bound depends on what score is being used to compute skill and what reference forecast is used, but the upper bound is always 1; 0 indicates no improvement over the reference forecast. The score used may be any of the common accuracy scores used in verification. For continuous variables, skill scores are usually based on either the mean absolute error or the mean squared error. For probability forecasts, skill scores are usually based on the Brier score.

The skill score has a range of -∞ to +1. A positive value of the skill score means the forecast is an improvement over the standard forecast. A negative value means that the forecast has lower accuracy than the standard forecast, and one might as well use the standard forecast instead.

4. Data sets used for the evaluation

4.1 Ocean Moored buoy Network for the Northern Indian Ocean (OMNI)

The Indian moored buoy network, the first of its kind in the Indian Seas, was established with the primary objective of supporting the cyclone and tsunami early warning services in the North Indian Ocean. The present buoy network (Figure 1) includes twelve (12) Ocean Moored buoy Network for the Northern Indian Ocean (OMNI) buoys with profile measurements (seven in the BoB and five in the AS) in deep waters, four coastal buoys, three tsunami buoys (one in AS and two in BoB) and one CALibration and VALidation (CAL-VAL) buoy, which is specifically deployed for the validation of satellite data (Venkatesan et al. 2016a). In addition, the Indian Arctic (IndARC) buoy has been maintained in the Arctic region since July 2014 (Venkatesan et al. 2016b). For the surface and sub-surface current comparison in the open ocean, we used OMNI buoy observations from twelve (12) locations over the Arabian Sea (AS) and the Bay of Bengal(BoB). The locations of these buoys are given in Figure 1.

4.2 Research Moored Array for African–Asian–Australian Monsoon Analysis and Prediction (RAMA)

The Research Moored Array for African–Asian–Australian Monsoon Analysis and Prediction (RAMA) is a Moored buoy Network part of the Indian Ocean Observing System (IndOOS) (Beal et al. 2020). As part of the in-situ network, for the Northern Indian Ocean OMNI forms the moored arrays in the tropical Indian Ocean. The mooring arrays offer an important backbone for the IndOOS, designed to provide new insights into ocean dynamics and for the investigation of air-sea interaction related to weather and climate events and their prediction, including cyclone tracking and marine heatwave events (Acharya and Chattopadhyay 2019; McPhaden et al. 2009). All moorings measure meteorological parameters at the sea surface (such as air temperature and surface wind speed), and ocean temperature, salinity, and currents at discrete depths in the upper few hundred meters of the ocean. A few sites at the equator also measure the ocean current profile in the upper hundred meters, while some other selected sites measure high-quality air-sea flux and/or biogeochemical variables.

4.3 The optimum interpolation (OI) sea surface temperature (OISST)

NOAA's Optimum Interpolation Sea Surface Temperature (OISST, also known as Reynolds' SST) is a global analysis product on a weekly at 1° grid and daily on a ¼° resolution (Reynolds et al. 2007). This SST analysis is a spatially gridded product created by interpolating and extrapolating data, resulting in a smoothed complete field. OISST provides global fields that are based on a combination of ocean temperature observations from satellite and in situ platforms (i.e., ships and buoys). These SST analyses are used in a range of applications including weather forecasting, climate studies, modeling, fisheries ecology, oceanography, and as a reference field for other satellite algorithms. There are two versions of the 1/4° daily OISST: "AVHRR-only" and "AVHRR+AMSR" are available. The AVHRR-only version uses satellite data from the infrared instrument, the Advanced Very High-Resolution Radiometer (AVHRR), and is available from 1981 onward. The temporal extent of AVHRR-only (>30 years) makes it desirable for climate studies. The AVHRR+AMSR version is available from July 2002 to October 2011 and was developed to incorporate additional data from the Advanced Microwave Scanning Radiometer on the EOS platform (AMSR-E). For this study, we used an AVHRR-only product to make robust daily climatology, which was used as a reference forecast for skill score computation. This data was also used for the spatial distribution of the SST forecast.

4.4 Sub-surface Temperature and Salinity from Argo

In order to evaluate MLD and D20, a three-dimensional observational temperature and salinity gridded product is needed. For the period of evaluation of models' MLD and D20 which is 2023, Mar to 2024 Mar, Argo only Roemmich Gilson climatology (Roemmich, D. and J. Gilson, 2009) is available. We have obtained the monthly mean fields of temperature and salinity available at https://sio-argo.ucsd.edu/RG_Climatology.html for the period 2023-2024. MLD is computed based on the density criterion of 0.125 change in sigma from the surface (Monterey and Levitus 1997).

4.5 Current

We assessed the spatial variability of first-day forecasted surface currents from ROMS and HYCOM by comparing them with the Ocean Surface Current Analysis-Real Time (OSCAR) product (Bonjean and Lagerloef, 2002). OSCAR surface currents are calculated from satellite datasets using a simplified physical model of an upper ocean turbulent mixed layer. The total velocity is comprised of a geostrophic term, a wind-driven term, and a thermal wind adjustment. Sikhakolli et al. (2013) evaluated the OSCAR current analysis over the Indian Ocean with buoy observation and showed that the zonal component of OSCAR-current is in good agreement with the corresponding component of buoy-observed current with a correlation exceeding 0.7, while the match between the meridional components is poorer. The RMSE over the eastern equatorial Indian Ocean shows very large ~ 50 cm/s for the zonal and ~ 20 cm/s for the meridional current. We also used surface and sub-surface current observation from OMNI buoy to evaluate the 1^{st}-day current forecast from ROMS and HYCOM.

4.6 Costal RADAR

Real-time coastal monitoring, rescue operations, and coastal current dynamics forecasting demand detailed maps of ocean surface currents. Satellite-based altimeters map the surface currents on a coarse spatial resolution often unable to detect the eddies and also have limited temporal resolution (several days) and assume that the observed flows are in geostrophic balance. Also, the currents closer to the coast (Land-Sea interface) are not reliable. The data availability from the satellite at a particular region mainly depends on satellite pass and hence they cannot provide near real-time continuous data needed for most of the applications. High frequency (HF) radars, in contrast, map the total surface currents (Geostrophic +Ekman + Eddies + Tides) at high spatio-temporal resolution up to offshore distance of about 200 km (Arunraj et al. 2018). Thus, the HF radars are found to be most suitable for measuring sea surface currents. These coastal HF radar data were used to evaluate the forecasted coastal currents from ROMS and HYCOM.

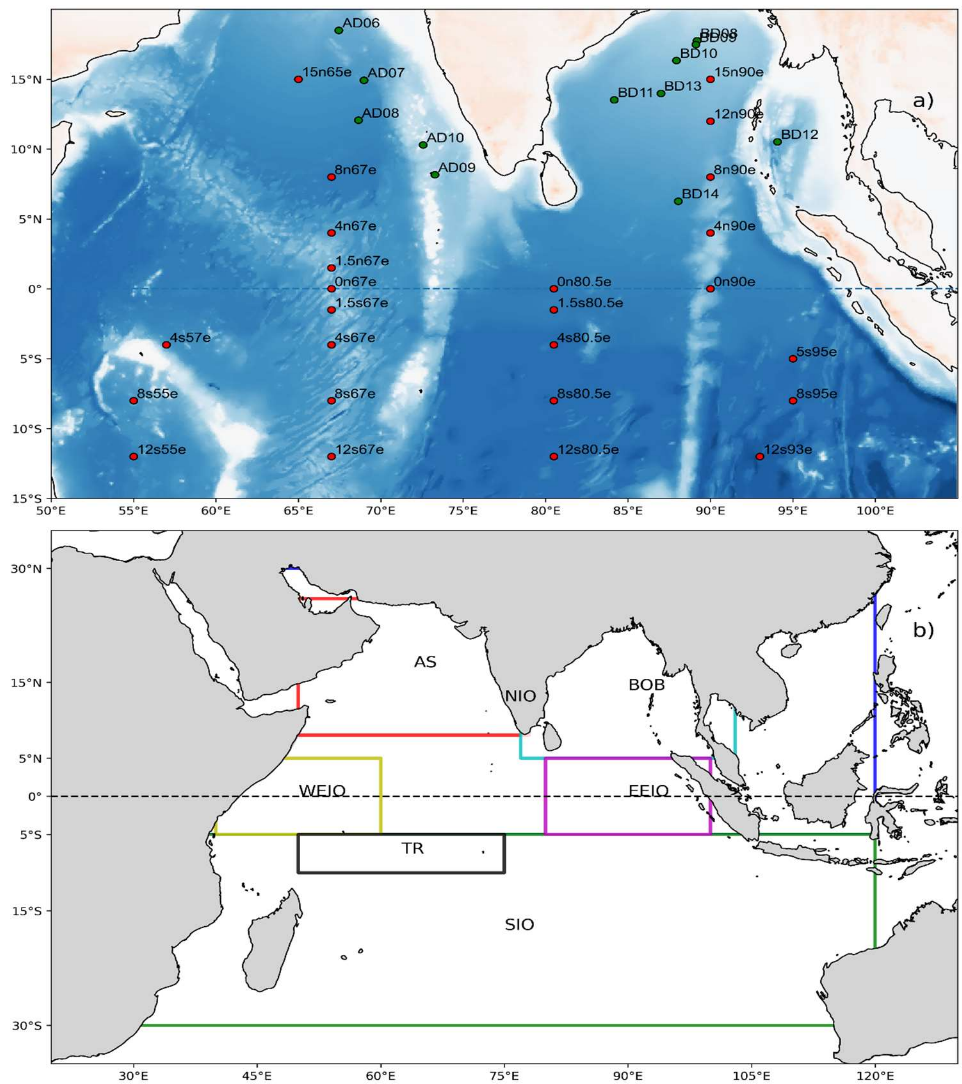

Figure 1: a) Locations of (a) RAMA, OMNI buoys (b) regions used for computing the region-wise forecast metrics. OMNI buoys are marked with AD and BD.

5. Evaluation results of the daily average first-day forecasted fields

5.1 Sea Surface Temperature (SST)

In order to see how good the first-day SST forecast was on a spatial scale, we used gridded ¼ degree SST products from Reynolds OISST (Reynolds et al. 2007). We computed spatial root mean square deviation (RMSD), correlation coefficients (CC), and standard deviation (STD) at each point over the entire Indian Ocean. Figure 2 shows the spatial RMSD of 1st day forecast. ROMS has higher RMSD across all regions except the Arabian Sea (AS) as compared to HYCOM. South of the equator ROMS, RMSD value ranged from 0.8 to 1 °C. RMSD shows a large value of ~ 1.7 °C near the southeast of Madagascar. Over the coastal regions of the Bay of Bengal (BoB), ROMS shows large values which is much less in HYCOM. However, in the Somali and Arabian coasts, RMSD is high in HYCOM as compared to ROMS. The CC values show greater than 0.9 for almost the entire basin both in HYCOM and ROMS, except in the eastern equatorial Indian Ocean where CC values are slightly low ~ 0.6 (Figure 3). This is reflected in the skill as well (see Figure 5d). The spatial distribution of ROMS STD is closer to the observed distribution as compared to HYCOM (Figure 4). We further selected a few boxes in the Indian Ocean such as AS, BoB, western equatorial Indian Ocean (WEIO), and eastern equatorial Indian Ocean (EEIO) (see in Figure 1b for the regions) and computed detailed statistics, which are shown in Figure 5. ROMS (HYCOM) shows systematic positive ~ 0.6 °C (negative) bias in all regions (Figure 5a). The CC values (>0.95) are also very high in all regions except in the EEIO where it is ~ 0.9 both in HYCOM and ROMS (Figure 5b). The RMSD values in all regions are less in HYCOM (0.2-0.5 °C) as compared to ROMS (0.4-0.8 °C) (Figure 5c). The skill score (SS) computed based on climatology (1982-2020) as the reference forecast in different regions is shown in Figure 5d. SS is positive in all regions and it is high in HYCOM as compared to ROMS, except in EEIO where ROMS shows negative SS. This implies ROMS 1st day SST forecast does not have any value addition over EEIO with reference to the OISST reference forecast.

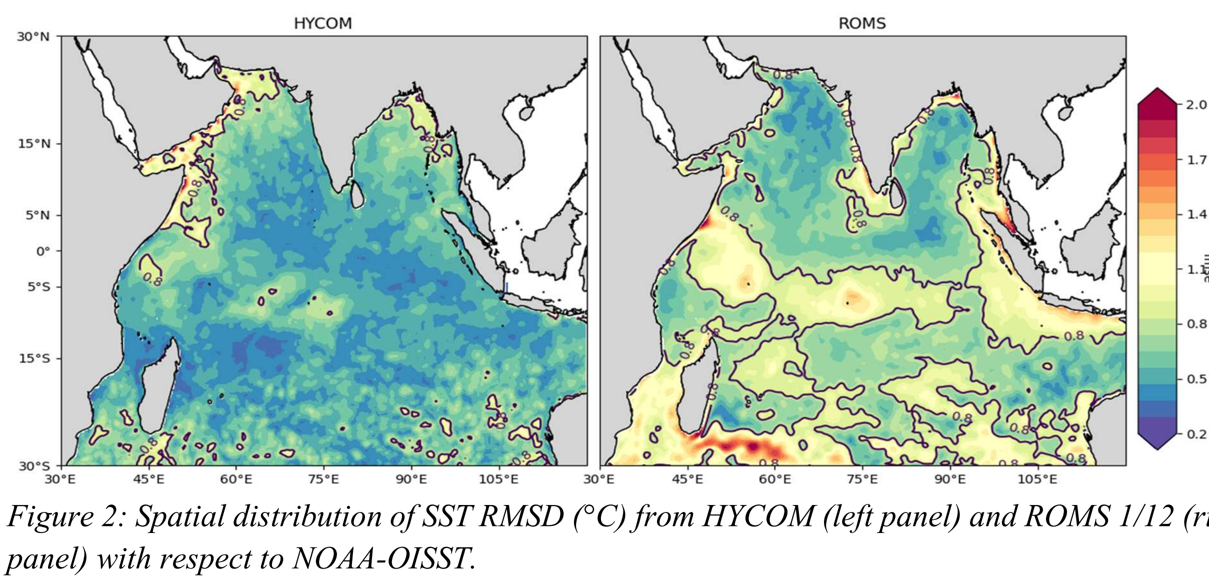

Figure 2: Spatial distribution of SST RMSD (°C) from HYCOM (left panel) and ROMS 1/12 (right panel) with respect to NOAA-OISST.

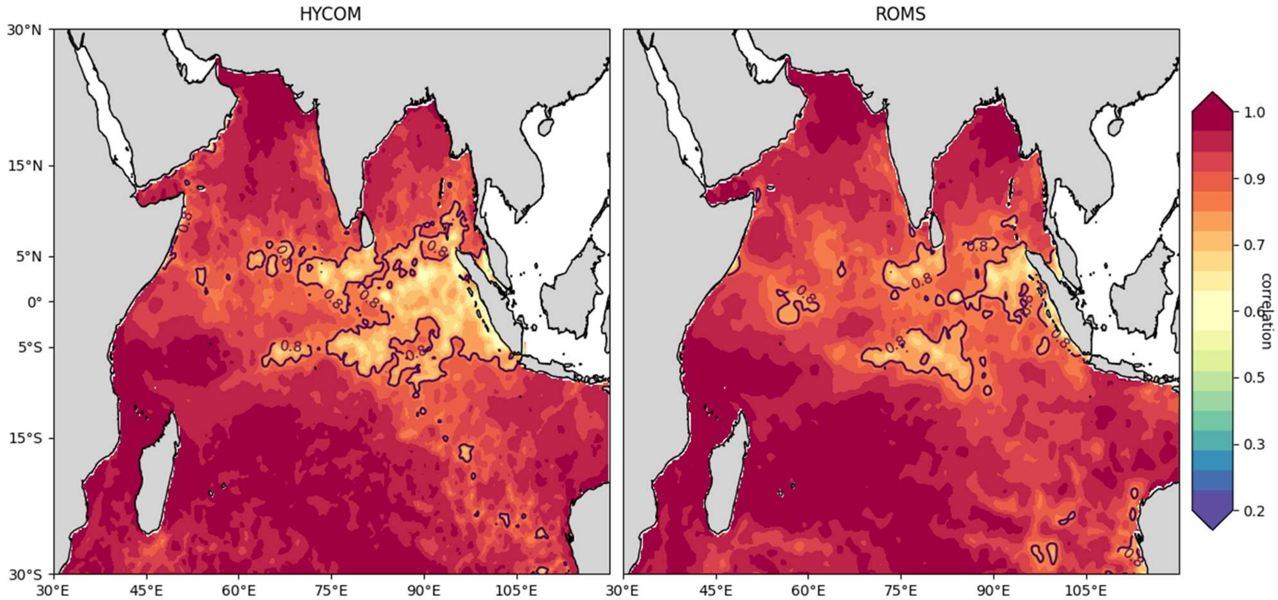

Figure 3: Daily SST spatial correlation from HYCOM (left panel) and ROMS 1/12 (right panel) with respect to NOAA-OISST.

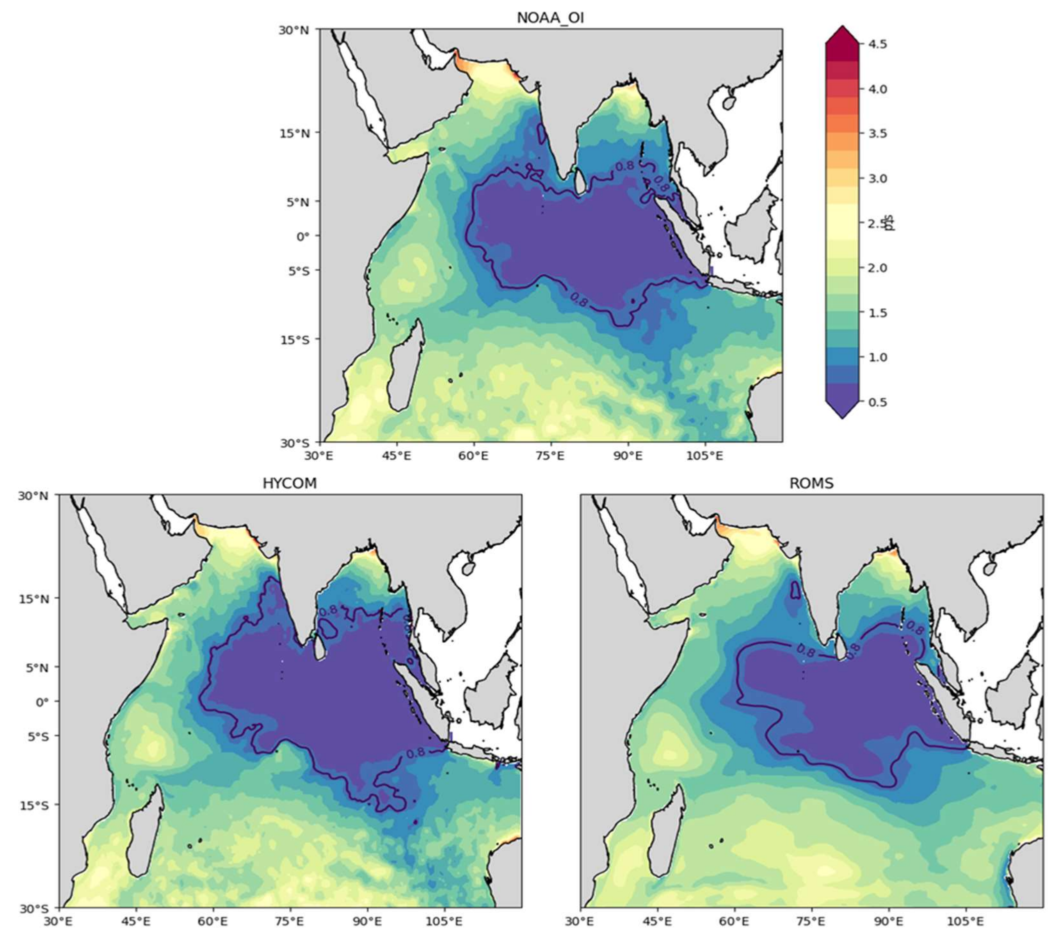

Figure 4: Spatial distribution of daily SST standard deviation (STD) (°C) from NOAA-OISST (top panel), HYCOM(bottom left panel), and ROMS 1/12 (bottom right panel).

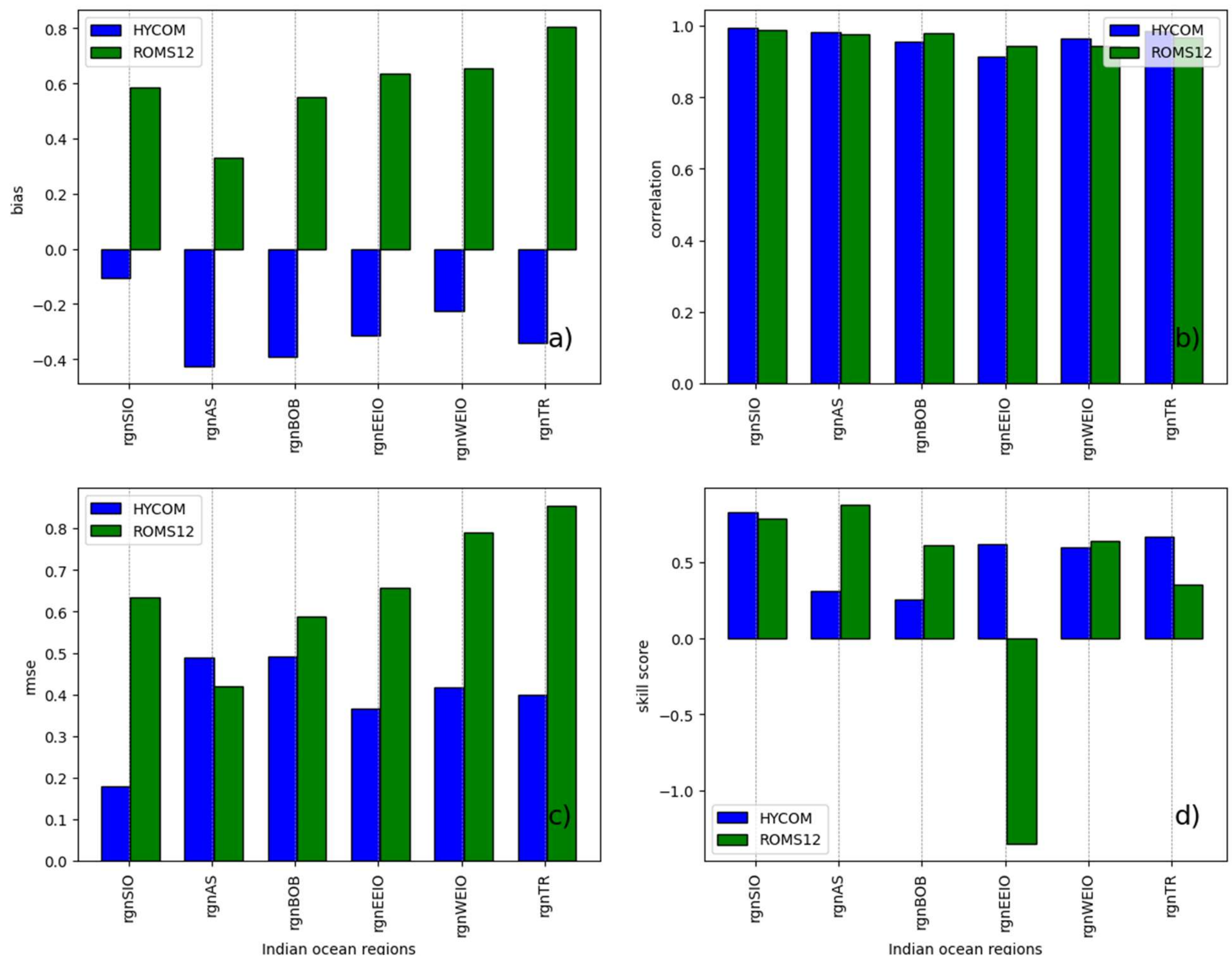

Figure 5: Region-wise forecast metrics for HYCOM and ROMS 1/12 (a) bias (°C),(b) correlation coefficient, (c) RMSE (°C), and (d) Skill Score with respect to NOAA-OISST observations.

We also compared the 1st-day forecast with RAMA (20 nos) and OMNI (10) buoy observations. However, many buoys show large data gaps hence for robust statistics we considered the buoy locations with more than 200 days data for 2020. We show 1st day SST forecast time series comparison of a few representative buoy locations over the AS, BoB, and western Equatorial IO in Figure 6. As already shown in Figure 5a, HYCOM (ROMS) under (overestimates) the daily 1st day SST forecast over the entire IO basin. The same thing can also seen in the time series plot as well (Figure 6). Neither HYCOM nor ROMS can capture the observed daily SST variability for these four (4) buoy locations. Both the model forecast is not able to capture the daily SST forecast with HYCOM slightly better matched with in-situ observation as compared to ROMS.

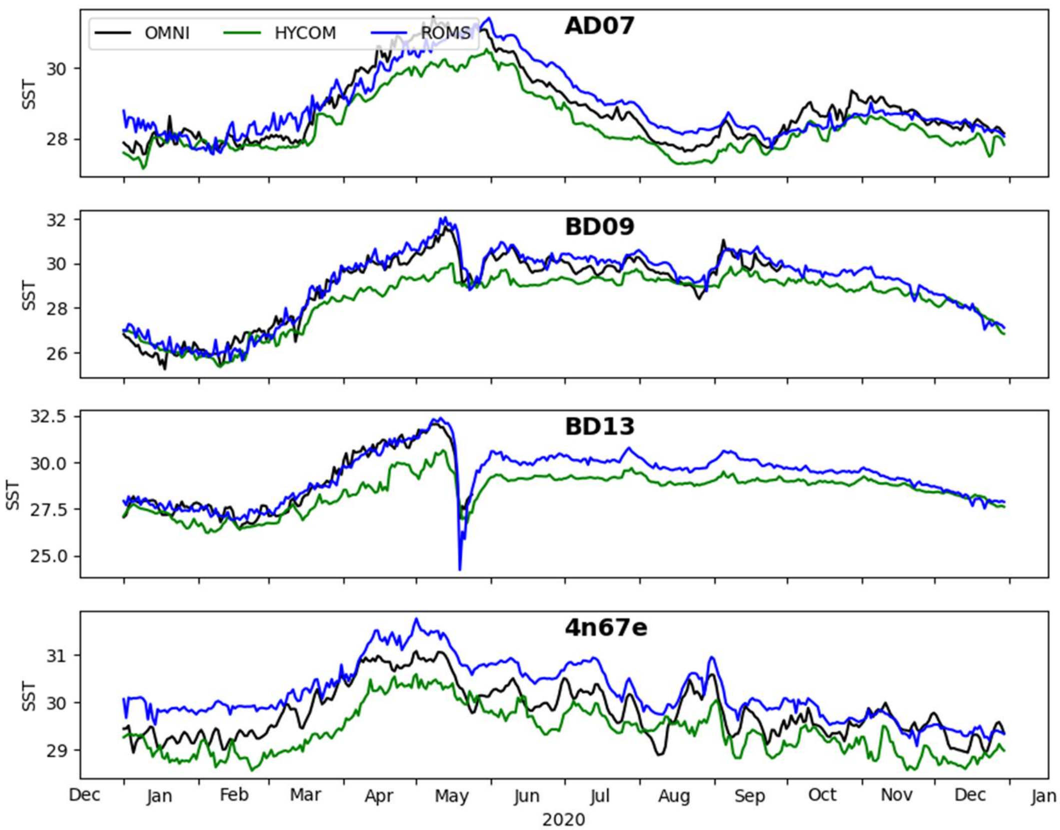

Figure 6: SST time series comparison of HYCOM and ROMS 1/12 at selected buoy locations AD07-Eastern Arabian Sea, BD09 and 13 Bay of Bengal and 4 °N 67 °E over southern Arabian Sea

Out of ten (10) OMNI buoys seven (7) show data availability of more than 200 days, hence we used these 7 OMNI buoys to show the bias, RMSE, and CC for each buoy in Figure 7. The same results of HYCOM under-estimated and ROMS over-estimated the annual mean 1st day SST forecast shown in figure 5 can also be seen in figure 7. But unlike the NOAA-OI SST comparison in which ROMS SST bias was more compared to HYCOM, with OMNI buoys ROMS bias is reduced in most of the buoys as compared to HYCOM. It's even < 0.1 °C at buoy location 18.5°N 67.5 °E and 14.9 °N, 69 °E for the ROMS, same for HYCOM its ~ 0.5 °C (Figure 7a). The CC values of HYCOM and ROMS 1stday SST forecast for all 7 buoy locations show>0.95 (Figure 7b). However, RMSE values in HYCOM ranged from 0.6-0.8 °C and in ROMS its 0.4-0.7 °C except for 4 °S 57 °E where it is ~ 0.9 for ROMS (Figure 7c). Overall OMNI buoy comparison shows ROMS 1st day SST forecast is slightly better than HYCOM. The slightly better overall statistics for ROMS can also seen in Table 1. Similar results can also be seen for the comparison with RAMA buoy locations in Figure 7. We show 14 buoy locations where more than 200 days of observed data is available. Compared to OMNI buoy locations biases and RMSE values are slightly more for both HYCOM and ROMS when used RAMA observations. But overall ROMS performance is slightly better than HYCOM (Figure 7 , Table 1 and Table 2).

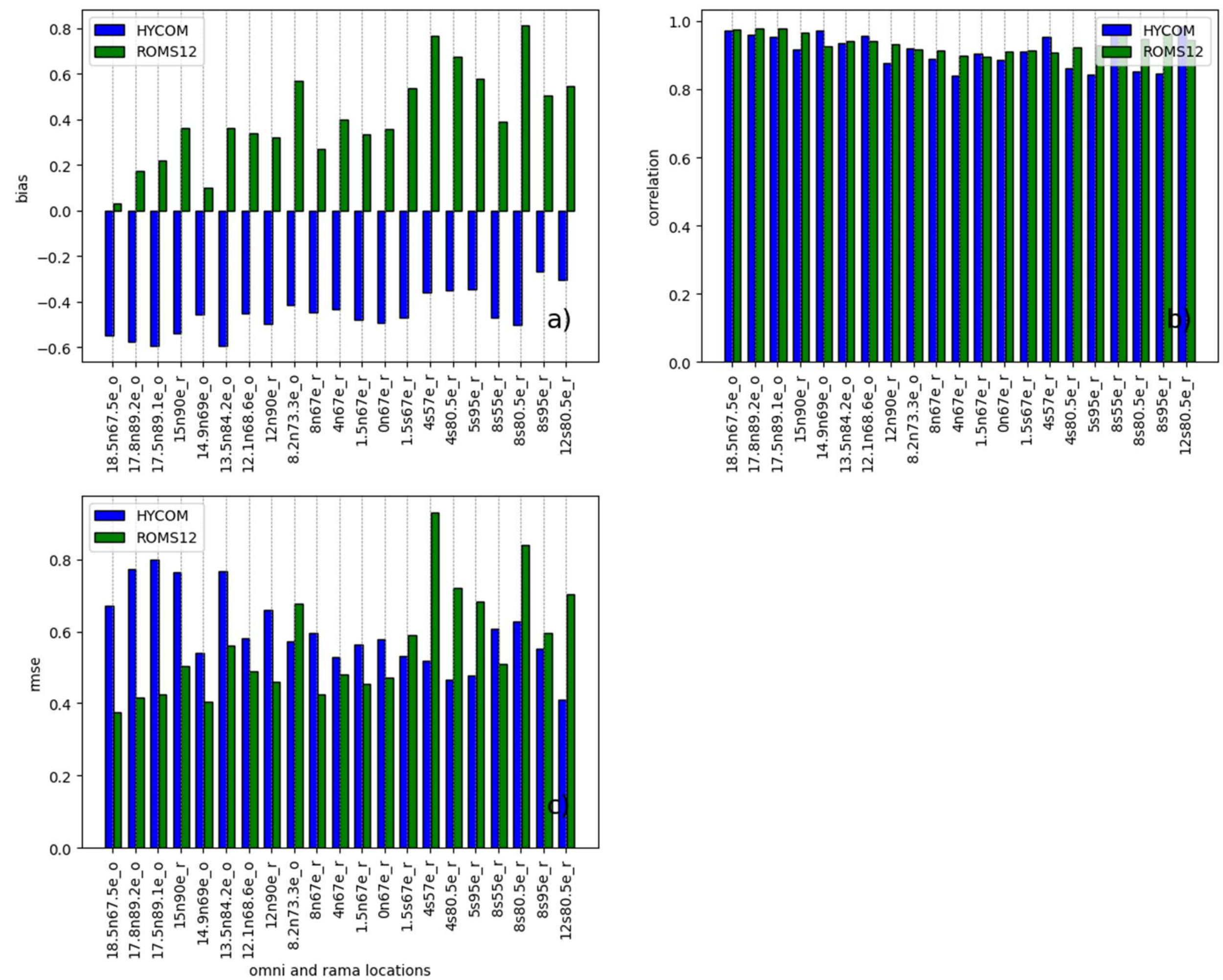

Figure 7:Location-wise statistics plots of SST with respect to OMNI and RAMA buoy observations (a)bias (°C), (b) correlation coefficient, and (c) RMSE (°C). All the metrics are for the year 2020 and the first-day forecast of ROMS 1/12 and HYCOM. Metric bars are plotted only if the number of good points is greater than 200. Buoy locations marked with o(r) in the X-axis are from OMNI(RAMA).

Table 1: SST forecast metrics at OMNI buoys.

	BIAS (°C)		CORR		RMSE(°C)		STD(°C)			SKILL SCORE		VALID POINTS
Buoy	HYCOM	ROMS	HYCOM	ROMS	HYCOM	ROMS	OBS	HYCOM	ROMS	HYCOM	ROMS	
18.5n67.5e_o	-0.55	0.03	0.97	0.98	0.67	0.38	1.61	1.44	1.72	0.17	0.74	347
14.9n69e_o	-0.46	0.1	0.97	0.93	0.54	0.4	1.04	0.86	0.97	0.5	0.72	365
12.1n68.6e_o	-0.45	0.34	0.96	0.94	0.58	0.49	1.05	0.79	0.97	0.22	0.45	364
8.2n73.3e_o	-0.41	0.57	0.92	0.92	0.57	0.68	0.89	0.63	0.9	0.53	0.35	365
10.3n72.6e_o	-0.26	0.24	0.02	0.05	0.32	0.37	0.15	0.68	1.04	0.59	0.44	59
17.8n89.2e_o	-0.58	0.17	0.96	0.98	0.77	0.42	1.66	1.25	1.64	0.36	0.81	293
17.5n89.1e_o	-0.59	0.22	0.96	0.98	0.8	0.42	1.65	1.21	1.56	0.35	0.82	273
13.5n84.2e_o	-0.59	0.36	0.94	0.94	0.77	0.56	1.24	0.87	1.15	-0.02	0.45	241
10.5n94.1e_o	-0.63	0.57	0.91	0.91	0.74	0.69	0.92	0.56	0.78	-1.76	-1.39	136
14n87e_o	-0.98	0.02	0.94	0.96	1.21	0.48	1.7	0.96	1.28	-0.59	0.75	145

Table 2: SST forecast metrics at RAMA buoys.

	BIAS (°C)		CORR		RMSE (°C)		STD (°C)			SKILL SCORE		VALID POINTS
Buoy	HYCOM	ROMS	HYCOM	ROMS	HYCOM	ROMS	OBS	HYCOM	ROMS	HYCOM	ROMS	
15n90e_r	-0.54	0.36	0.92	0.97	0.76	0.5	1.35	1.23	1.28	-0.14	0.51	333
12n90e_r	-0.5	0.32	0.88	0.93	0.66	0.46	0.91	0.76	0.88	-0.06	0.49	365
8n67e_r	-0.45	0.27	0.89	0.91	0.6	0.42	0.81	0.55	0.73	0.31	0.65	327
8n90e_r	-0.34	0.91	0.06	0.01	0.38	0.93	0.11	0.47	0.61	-2.8	-21.39	52
4n67e_r	-0.43	0.4	0.84	0.9	0.53	0.48	0.55	0.51	0.6	0.5	0.59	365
1.5n67e_r	-0.48	0.34	0.9	0.9	0.57	0.45	0.67	0.52	0.66	0.55	0.71	359
0n67e_r	-0.49	0.36	0.89	0.91	0.58	0.47	0.65	0.59	0.75	0.4	0.61	365
0n80.5e_r	-0.42	0.36	-0.32	-0.4	0.48	0.45	0.1	0.51	0.56	0.43	0.49	23
0n90e_r	-0.51	0.42	0.84	0.91	0.59	0.48	0.53	0.36	0.55	0.47	0.65	159
1.5s67e_r	-0.47	0.54	0.91	0.91	0.53	0.59	0.6	0.69	0.83	0.59	0.49	319
1.5s80.5e_r	-0.6	0.58	0.88	0.91	0.66	0.62	0.5	0.52	0.64	0.42	0.49	134
4s57e_r	-0.36	0.77	0.96	0.91	0.52	0.93	1.25	1.15	1.12	0.68	-0.05	365
4s67e_r	-0.52	0.62	0.58	0.83	0.57	0.64	0.25	0.81	0.8	0.82	0.78	15
4s80.5e_r	-0.35	0.67	0.86	0.92	0.47	0.72	0.58	0.42	0.66	0.61	0.07	365
5s95e_r	-0.34	0.58	0.84	0.93	0.48	0.68	0.61	0.49	0.85	0.66	0.31	356
8s55e_r	-0.47	0.39	0.97	0.98	0.61	0.51	1.48	1.53	1.59	0.67	0.77	365
8s67e_r	-0.55	0.96	0.79	0.89	0.59	0.97	0.25	0.97	0.91	0.34	-0.8	18
8s80.5e_r	-0.5	0.81	0.85	0.95	0.63	0.84	0.67	0.6	0.61	0.39	-0.1	230
8s95e_r	-0.27	0.5	0.85	0.96	0.55	0.6	0.85	0.69	1.08	0.6	0.53	267
12s80.5e_r	-0.3	0.55	0.98	0.94	0.41	0.7	1.35	1.05	1.09	0.85	0.55	274

We computed skill score (SS) based on Murphy's (1993) formula (see equation 2 in section 3). The SS values are very sensitive to the reference forecast which is generally used as a long-term mean climatology. If the SS values are positive then any forecasted fields have some value. SS value of 1 is a perfect forecast. Since the climatology of OMNI daily SST for the different buoy locations underrepresents the daily values due to large data gaps, we used standard deviation methods for such cases and also 40 years of climatology from OI SST as a reference forecast. The SS computed with these three methods is shown in Figure 8. It can be seen with OMNI SST as a reference, SS values are mostly negative for HYCOM in all 7 OMNI buoy locations but ROMS shows positive SS values over 18.5 °N,67.5 °E, 17.8 °N 89.2 °E, 17.2 °N, 89.1 °E and 8 °S, 55 °E buoy locations (Figure 8a). SS values become positive for both ROMS and HYCOM over most of the buoy locations when STD values from buoy observations are used as reference. SS values are slightly higher in ROMS as compared to HYCOM with a range of (0.4-0.9) (Figure 8b). When OI SST is used as a reference forecast again all values are positive and ROMS SS values are much higher than HYCOM in all OMNI buoy locations. The ROMS SS values ranged from 0.2-0.8 whereas for HYCOM these values were 0.2-0.5 with a negative value over 15 °N 90 °E. When repeating this with 14 RAMA buoys HYCOM SS values show higher than ROMS over most of the locations. But at 8 °S 80.5 °E ROMS SS values show negative which also falls over the EEIO where ROMS SS values also show negative. Hence, it can be concluded that over the EEIO 1st day SST forecast does not have any valued skill for ROMS.

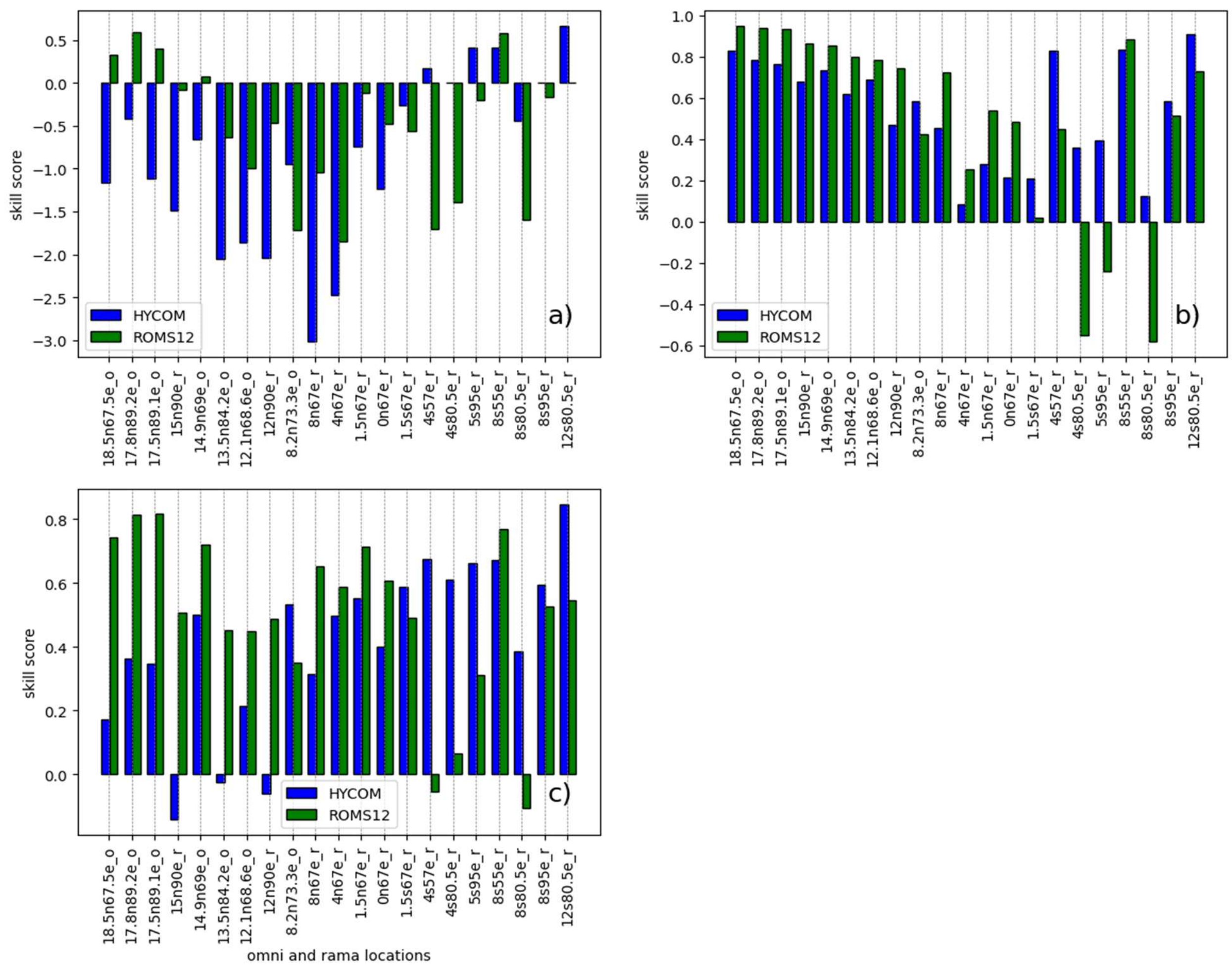

Figure 8: Skill scores of HYCOM and ROMS 1/12 SST computed using different reference forecasts (a) observational climatology from OMNI and RAMA buoy observations (b) observational standard deviation from respective OMNI and RAMA buoy observations and (c) NOAA-OI SST at OMNI and RAMA buoy locations.

5.2 Surface Current Comparison

Accurate prediction of ocean currents is important for maritime safety, hazardous chemical spills, fisheries, the oil and gas industry, and national security. Information on currents is used for search and rescue, for tracking of oil spills, safe navigation, shipping and naval operations, design of port and coastal infrastructure, and for safe recreational activities. INCOIS is providing 5-day advance current forecast based on ROMS and HYCOM (see the details in sec 2). Similar to SST forecast evaluation, we used OSCAR surface current as well as in-situ buoy observation to evaluate the 1st day current forecast from ROMS and HYCOM.

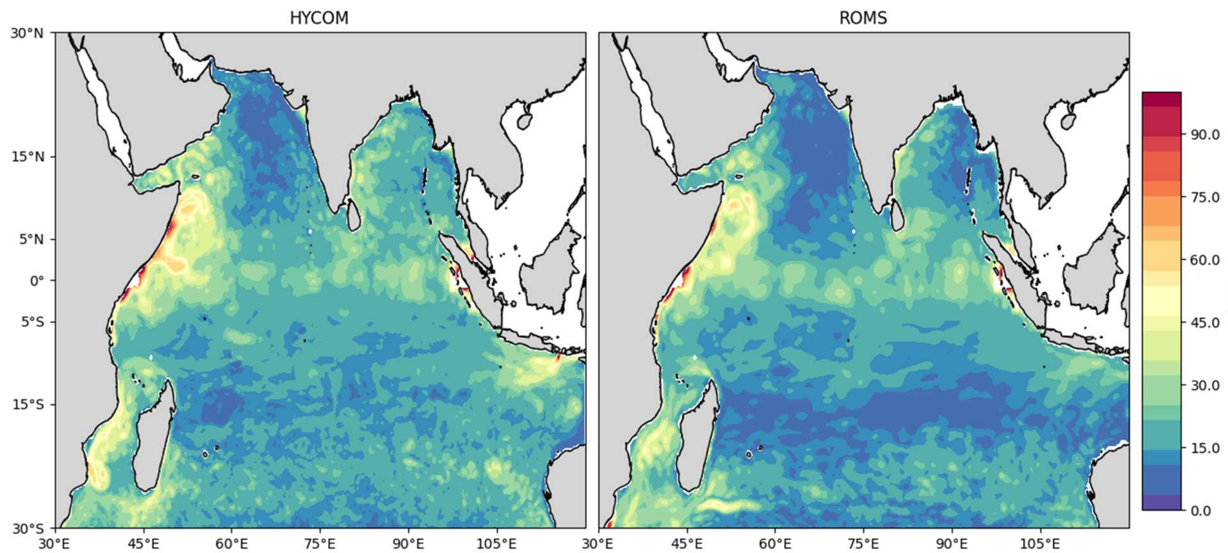

Figure 9: Current Speed RMSE (cm/s) computed with respect to OSCAR analysis for HYCOM (left panel) and ROMS 1/12 (right panel)

Figure 9 shows the spatial distribution of 1st-day surface current speed forecast RMSE values computed with respect to OSCAR analysis over the entire Indian Ocean. The RMSE values are ~ 10 cm/s over AS ~ 20 cm/s over BoB and slightly higher in the equatorial Indian Ocean (~ 40 cm/s). RMSE values are high over the Somali coast where it shows RMSE values as large as 80 cm/s for both ROMS and HYCOM forecast. Overall basin-wide ROMS RMSE values are slightly lower as compared to HYCOM. However, the spatial distribution of high CC values ~ 0.5-0.8 is more in HYCOM as compared to ROMS (Figure 10). Daily variability (STD) in ROMS shows closer to OSCAR values as compared to HYCOM (Figure 11). Region-wise bias, CC, RMSE, and SS can be seen in Figure 12. HYCOM shows stronger currents in all regions with a positive bias of 3-5 cm/s except over the EEIO where it shows a weaker current with a bias of 10 cm/s (Figure 12a). ROMS shows weaker currents in all regions as compared to OSCAR (Figure 12a). CC values are also higher in HYCOM as compared to ROMS (Figure 12b). RMSE values over the equatorial regions are high for both ROMS and HYCOM (Figure 12c). Overall HYCOM RMSE values are lower than ROMS. Both ROMS and HYCOM show positive SS in all regions with values ranged 0.5-0.9. ROMS shows higher skill over SIO, BoB, and WEIO regions. However, over AS and EEIO HYCOM shows higher skill as compared to ROMS (Figure 12d).

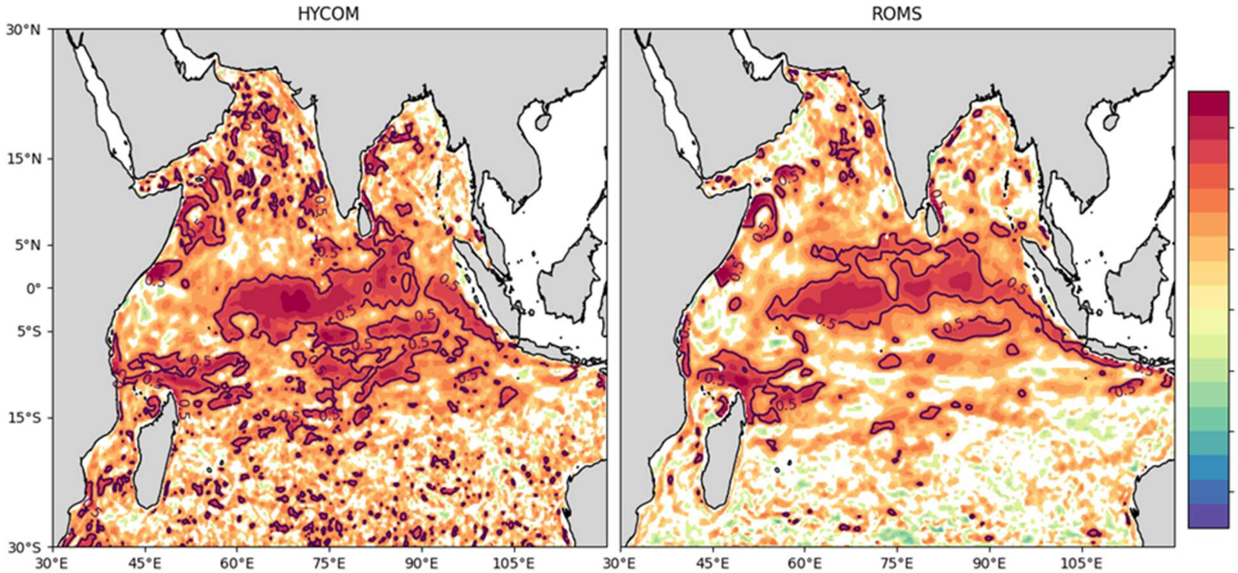

Figure 10: Current Speed correlation coefficient computed with respect to OSCAR analysis for HYCOM (left panel) and ROMS 1/12(right panel)

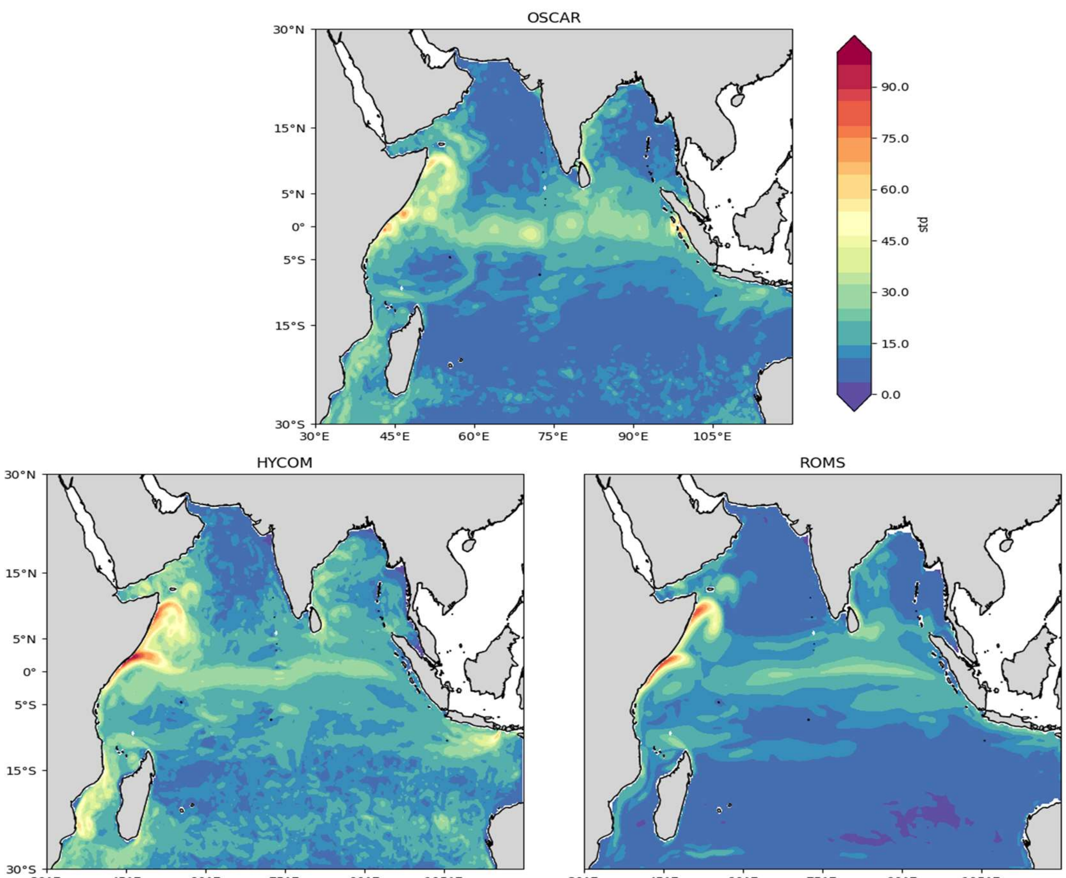

Figure 11: Daily standard deviation (STD)(cm/s) of surface currents from OSCAR analysis(upper panel), HYCOM (lower left panel), and ROMS 1/12 (lower right panel).

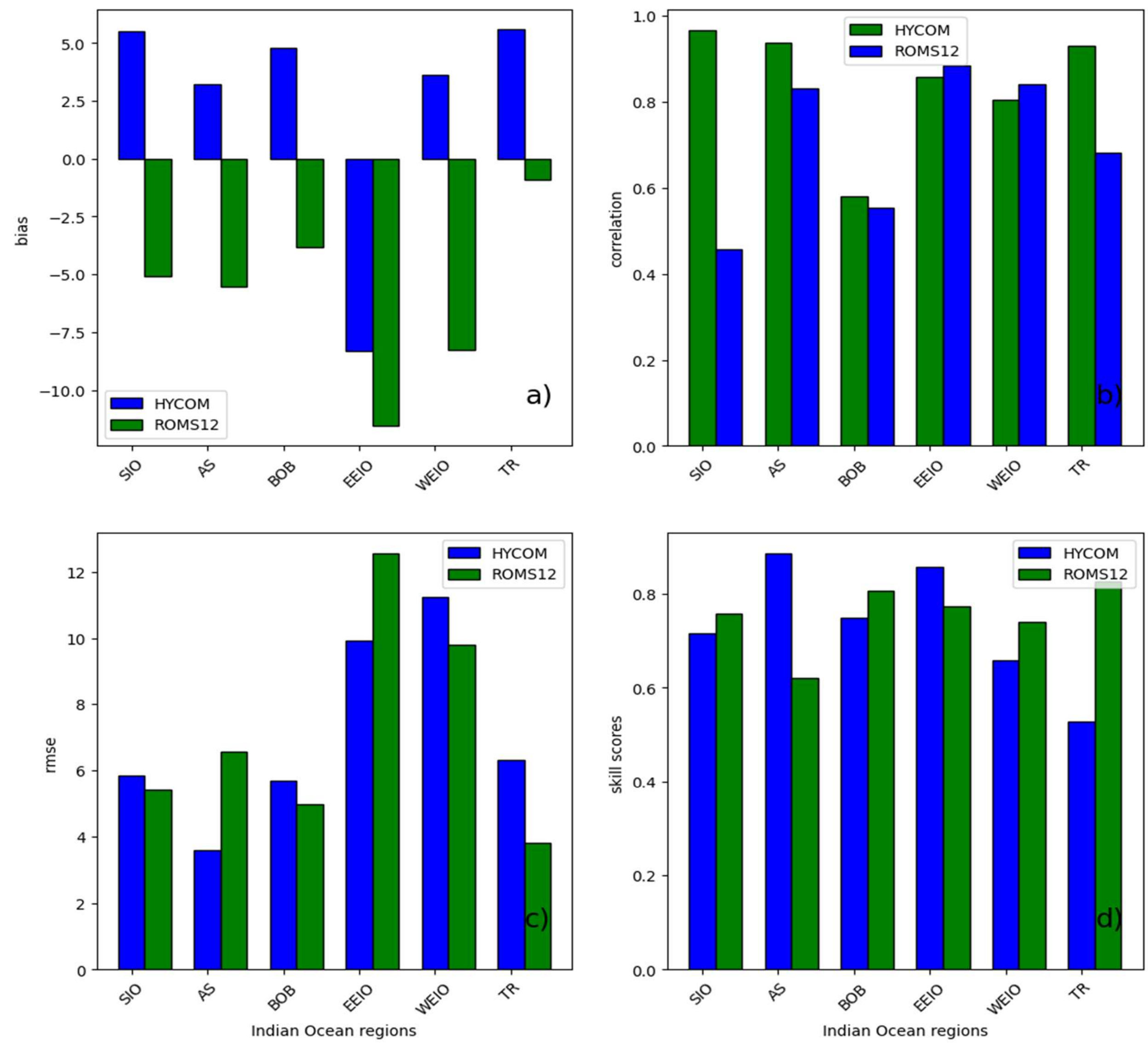

Figure 12: Region-wise current speed forecast metrics for HYCOM and ROMS1/12 (a) bias (cm/s), (b) correlation coefficient, (c) RMSE (cm/s), and (d) Skill Score with respect to OSCAR reference climatology.

Similar to the SST, we evaluated the 1st day-forecasted current speed with OMNI and RAMA buoys as well. We used 8 OMNI and 5 RAMA buoys for the bias, CC, RMSE, and SS with more than 200 days of data. Figure 13 shows bias, CC, and RMSE from the OMNI and RAMA buoy locations. Similar to Figure 12 with respect to OSCAR comparisons, with buoy observations too, ROMS current shows negative bias ~ (2-12) cm/s i,e weaker than buoy for all locations. HYCOM shows mixed i.e., positive and negative bias but with much lower values ~ 2-5 cm/s (Figure 13a). CC values ranged between 02-0.5 for both ROMS and HYCOM with a few locations where ROMS performed better (Figure 13b). RMSE values for both the ROMS and HYCOM show similar in all buoy locations and ranged between ~ (7-24) cm/s (Figure 13c). Similar to SST, for the RAMA buoy locations, all these values are high as compared to OMNI buoy locations (Figure 13). The SS with reference forecast as OMNI buoy climatology, STD, and daily OSCAR climatology made from 1992-2022 is shown in Figure 14. It can be seen that with buoy climatology and STD as reference forecasts both ROMS and HYCOM SS show negative except at 1.5 °N, 67 °E, and 17.5 °N,89.1 °E where ROMS shows positive skill. Similarly, HYCOM at 18.5°N , 67.5°E and 10.3 °N,72.6 °E show slight positive skill. However, with OSCAR climatology as a reference forecast SS values show positive values in all buoy locations with slightly better skill in ROMS. Similar results can be seen in 5 RAMA buoy locations as well.

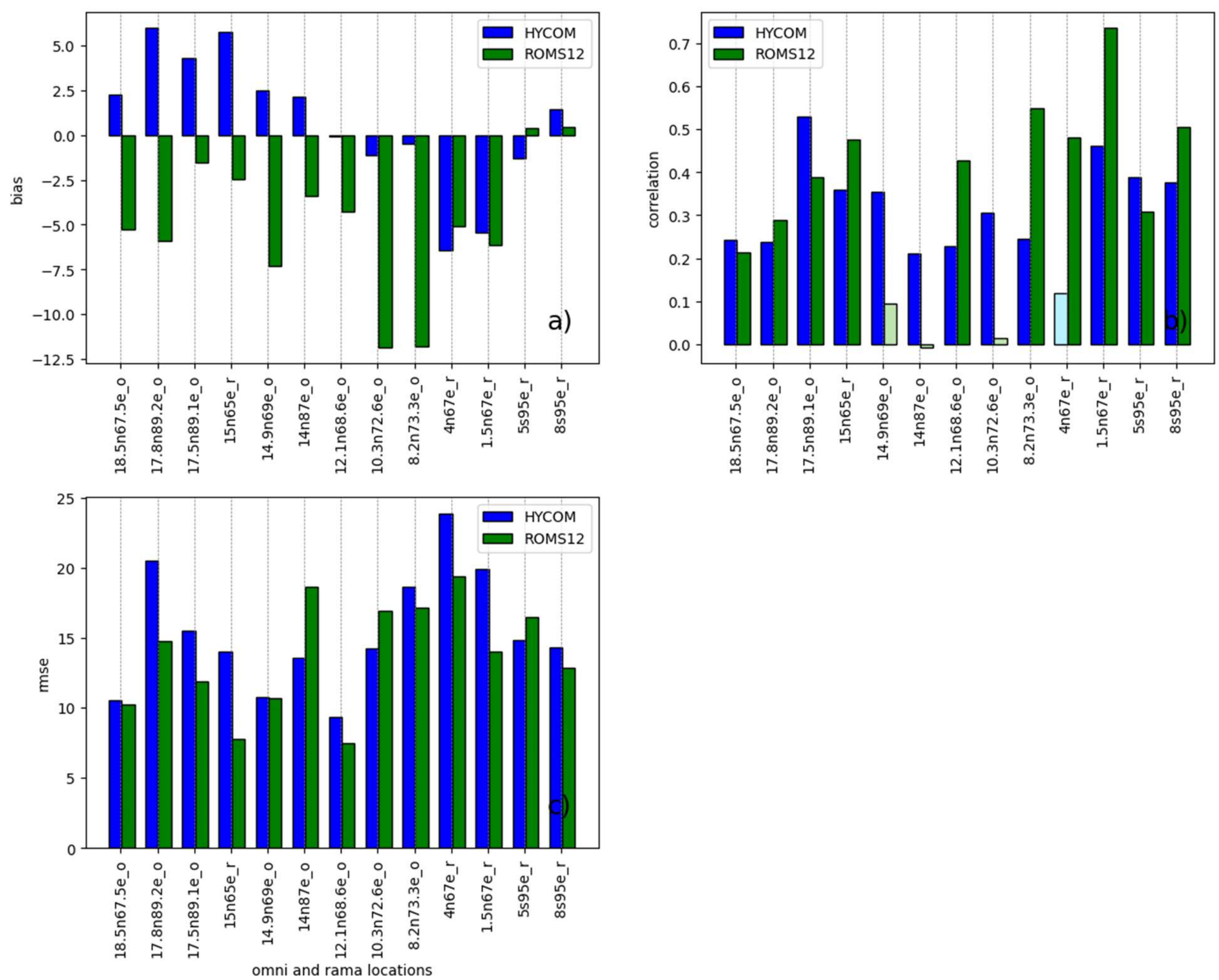

Figure 13: Location-wise statistics plots of surface current speed with respect to OMNI and RAMA buoy observations (a)bias (cm/s), (b) correlation coefficient, and (c) RMSE (cm/s). All the metrics are for the year 2020 and the first-day forecast of ROMS 1/12 and HYCOM. Metric bars are plotted only if the number of good points is greater than 200. Buoy locations marked with o(r) in the X-axis are from OMNI(RAMA).

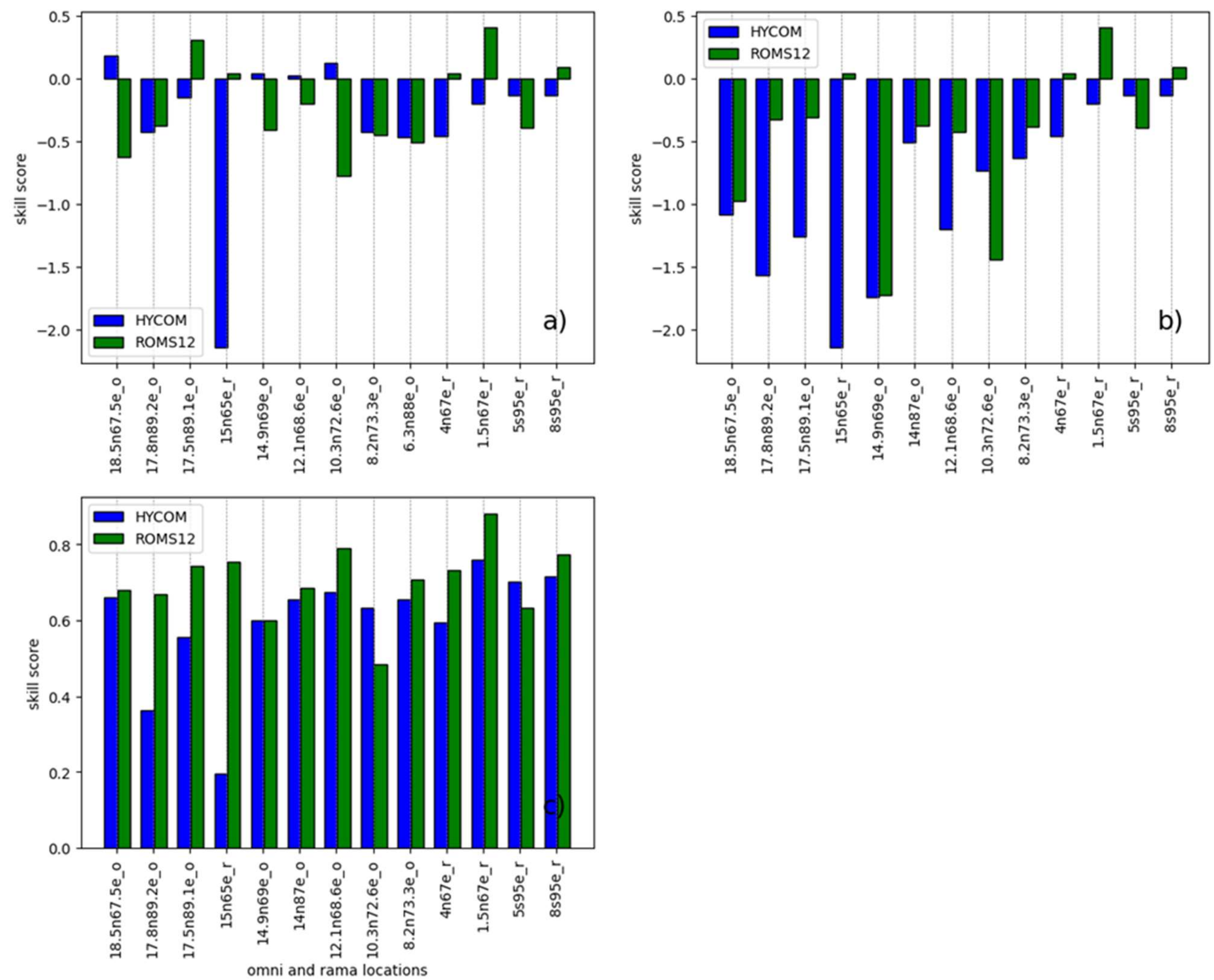

Figure 14: Skill Scores of HYCOM and ROMS 1/12 surface current computed using different reference forecasts (a) observational climatology (b) observational standard deviation and (c) OSCAR daily analysis as reference forecast

Time series comparison of surface current speed (15 m) at BD08 and BD14 locations both are in the BoB (see Figure 1a) shown in Figure 15. Both ROMS and HYCOM are unable to capture the buoy observed daily current speed variability at BD08 location which is located in the northern BoB. Almost throughout the year, HYCOM(ROMS) over (under) estimated the buoy's observed current speed. HYCOM shows spurious strong current during Nov-Dec which is absent in buoy observation and also in ROMS. Daily observed variability at the southern BoB buoy location at BD14, was captured reasonably well by both ROMS and HYCOM 1st day forecast. Similar to north BoB, the observed current speed variability is not captured by both ROMS and HYCOM over the Arabian Sea (AD07 and AD09 in Figure 15). At the RAMA buoy location over the central equatorial Indian Ocean, the 1st day FC of ROMS shows a reasonably good match with buoy observation with HYCOM underperforming slightly as compared to ROMS (1.5n67e Figure

16). However, over the central Arabian Sea RAMA buoy location both ROMS and HYCOM perform similarly to that of BoB and AS. The statistics of zonal current comparisons

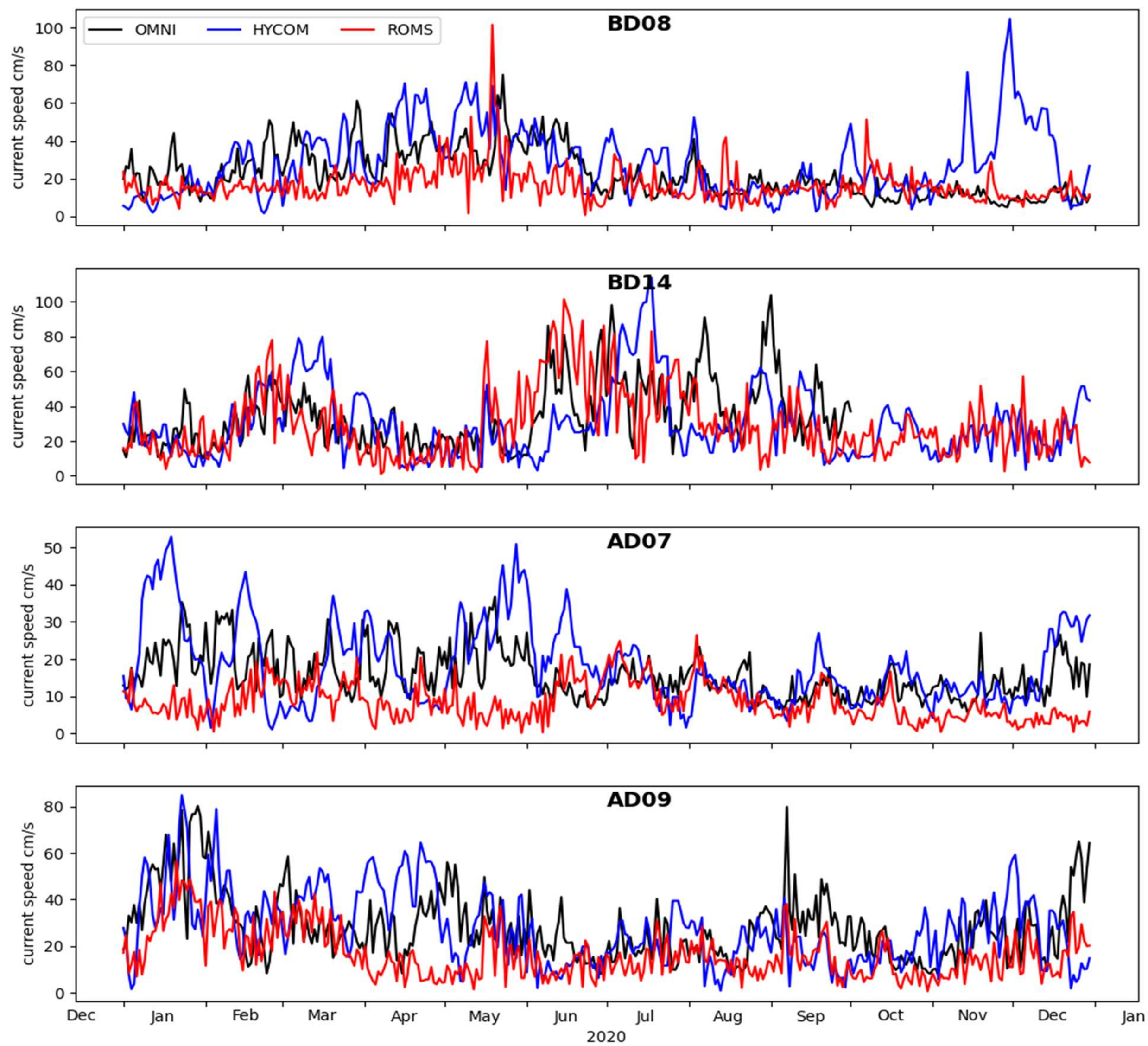

Figure 15: Surface Current speed (15 m depth) comparison at two locations (BD08, BD14) in the BoB and two locations in the AS (AD07, AD09)

with OMNI buoys are shown in Table 3. ROMS performs slightly better than HYCOM in terms of bias, CC, STD, and RMSE. Similar results can be seen for the RAMA buoys as well (Table 4). Statistics for current speed are shown in Tables 5 and 6 and it shows similar results to that of zonal current. EICC and WICC are two seasonally reversing currents along the east and west coasts of India. In order to see how good the forecast is at detecting the EICC and WICC we compared 1st day forecasted surface current with daily OSCAR analysis is shown in Figure 17. Annual mean current speed over the western BoB was overestimated in HYCOM and underestimated in ROMS. However, the spatial pattern is well captured in HYCOM as compared to ROMS. EICC structure in HYCOM again shows closer to OSCAR analysis as compared to ROMS (middle panel of Figure

18). ROMS current underestimates the EICC and also despite being eddy-resolving it could not capture the positions of cyclonic and anti-cyclonic eddies seen in the SLA observation (see Figure 19).

Table 3: Zonal current forecast metrics at OMNI buoys

	BIAS (cm/s)		CORR		RMSE(cm/s)		STD (cm/s)			SKILL SCORE		VALID POINTS
Buoy	HYCOM	ROMS	HYCOM	ROMS	HYCOM	ROMS	OBS	HYCOM	ROMS	HYCOM	ROMS	
18.5n67.5e_o	-3.33	-0.1	0.43	0.31	15.9	13.69	14	13.28	7.09	-0.29	0.05	220
14.9n69e_o	2.87	6.5	0.51	0.42	13.19	12.79	12.09	13.8	5.87	-0.05	0.02	365
12.1n68.6e_o	-3.77	-1.54	0.44	0.29	13.18	11.38	11.47	12.39	6.04	-0.19	0.12	364
8.2n73.3e_o	2.77	5.25	0.34	0.38	22.9	19.9	19.97	19.7	12.64	-0.27	0.04	365
10.3n72.6e_o	1.5	-7.88	0.47	-0.02	15.33	18.51	15.38	17.71	6.42	0.19	-0.18	278
17.8n89.2e_o	-10.44	-0.7	0.34	0.29	25.8	14.63	14.58	24.15	8.65	-1.06	0.34	365
17.5n89.1e_o	-1.02	8.56	0.29	0.36	18.98	16.12	13.51	20.76	10.26	-0.79	-0.29	282
10.5n94.1e_o	-23.93	-16.68	0.1	0.25	34.81	25.21	19.17	22.29	11.68	-1.3	-0.2	136
14n87e_o	1.81	-2.58	0.17	0.22	18.01	14.45	13.33	19.09	11.83	-0.67	-0.08	145
6.3n88e_o	-5.79	8.17	0.6	0.55	27.4	30.05	30.76	27.8	27.53	0.25	0.1	275

Table 4: Zonal current forecast metrics at RAMA buoys

	BIAS (cm/s)		CORR		RMSE(cm/s)		STD(cm/s)			SKILL SCORE		
Buoy	HYCOM	ROMS	HYCOM	ROMS	HYCOM	ROMS	OBS	HYCOM	ROMS	HYCOM	ROMS	VALID POINTS
15n65e_r	-5.68	-2.09	0.21	0.64	14.71	8.15	10.22	10.47	6.93	-0.41	0.57	225
4n67e_r	1.59	-2.4	0.35	0.78	29.08	19.01	28.94	20.96	25.47	0.04	0.59	269
1.5n67e_r	5.5	-2.71	0.81	0.89	21.92	16.51	36.1	29.43	31.17	0.63	0.79	291
0n67e_r	23.75	1.07	0.91	0.94	27.07	16.07	27.86	42.27	43.72	0.04	0.66	158
0n80.5e_r	14.04	-19.12	0.95	0.85	19.13	25.83	32.01	42.06	40.19	0.77	0.58	17
0n90e_r	6.81	8.4	0.94	0.87	32.25	28.44	29.01	42.93	37.67	-0.11	0.14	159
4s57e_r	19.21	24.71	0.27	0.17	24.54	26.38	3.97	24.7	18.14	-37.31	-43.28	61
5s95e_r	11.1	15.03	0.05	-0.07	26.9	30.65	15.35	21.73	23.77	-1.77	-2.6	309
8s55e_r	-15.23	25.67	0.65	0.69	21.12	29.21	19.35	14.27	21.59	-0.14	-1.19	59
8s95e_r	5.67	5.03	0.05	-0.11	25.68	30.16	17.34	20.05	24.41	-0.97	-1.71	243

Table 5: Current speed forecast metrics at OMNI buoys

	BIAS (cm/s)		CORR		RMSE(cm/s)		STD(cm/s)			SKILL SCORE		VALID POINTS
Buoy	HYCOM	ROMS	HYCOM	ROMS	HYCOM	ROMS	OBS	HYCOM	ROMS	HYCOM	ROMS	
18.5n67.5e_o	2.23	-5.28	0.24	0.21	10.49	10.21	7.26	9.2	6.17	0.66	0.68	220
14.9n69e_o	2.52	-7.3	0.35	0.1	10.73	10.7	6.47	10.79	5.05	0.6	0.6	365
12.1n68.6e_o	-0.09	-4.28	0.23	0.43	9.3	7.48	6.26	8.43	5.03	0.67	0.79	364
8.2n73.3e_o	-0.48	-11.8	0.25	0.55	18.63	17.17	14.56	15.71	10.65	0.66	0.71	365
10.3n72.6e_o	-1.13	-11.86	0.3	0.01	14.29	16.93	10.84	17	5.43	0.63	0.48	278
17.8n89.2e_o	5.97	-5.92	0.24	0.29	20.51	14.75	12.79	18.21	9.4	0.36	0.67	365
17.5n89.1e_o	4.33	-1.52	0.53	0.39	15.56	11.85	10.35	16.34	10.48	0.56	0.74	282
10.5n94.1e_o	-2.4	-18.19	-0.1	0.03	15.86	20.99	9.09	14.1	7.68	0.71	0.5	136
14n87e_o	2.13	-3.42	0.21	-0.01	13.58	18.64	8.33	11.58	13.75	0.46	-0.02	145
6.3n88e_o	-3.04	-3.75	0.37	0.41	23.28	22.28	18.96	20.11	19.49	0.66	0.69	275

Table 6: Current speed forecast metrics at RAMA buoys

	BIAS (cm/s)		CORR		RMSE(cm/s)		STD(cm/s)			SKILL SCORE		VALID POINTS
Buoy	HYCOM	ROMS	HYCOM	ROMS	HYCOM	ROMS	OBS	HYCOM	ROMS	HYCOM	ROMS	
15n65e_r	5.78	-2.49	0.36	0.48	14.06	7.75	7.93	11.8	5.92	0.2	0.76	225
4n67e_r	-6.46	-5.11	0.12	0.48	23.89	19.38	19.77	16.48	15.47	0.59	0.73	269
1.5n67e_r	-5.45	-6.17	0.46	0.73	19.97	14.06	18.22	18.73	15.39	0.76	0.88	291
0n67e_r	7.3	8.48	0.75	0.84	19.67	15.39	17.46	28.23	24.67	0.58	0.74	158
0n80.5e_r	8.99	-8.15	0.88	0.74	16.68	14.33	17.45	25.77	25.5	0.85	0.89	17
0n90e_r	27.17	16.34	0.9	0.83	33.09	26.78	21.03	28.31	26.45	-0.08	0.29	159
4s57e_r	25.45	22.28	0.26	0.19	28.49	23.94	2.32	18.3	14.06	-26.86	-18.67	61
5s95e_r	-1.32	0.37	0.39	0.31	14.87	16.51	13.96	14.33	16.21	0.7	0.63	309
8s55e_r	-0.69	10.18	0.08	-0.12	15.78	21.52	12.68	11.17	12.32	0.61	0.27	59
8s95e_r	1.43	0.43	0.38	0.51	14.36	12.84	13.49	11.81	14.04	0.72	0.77	243

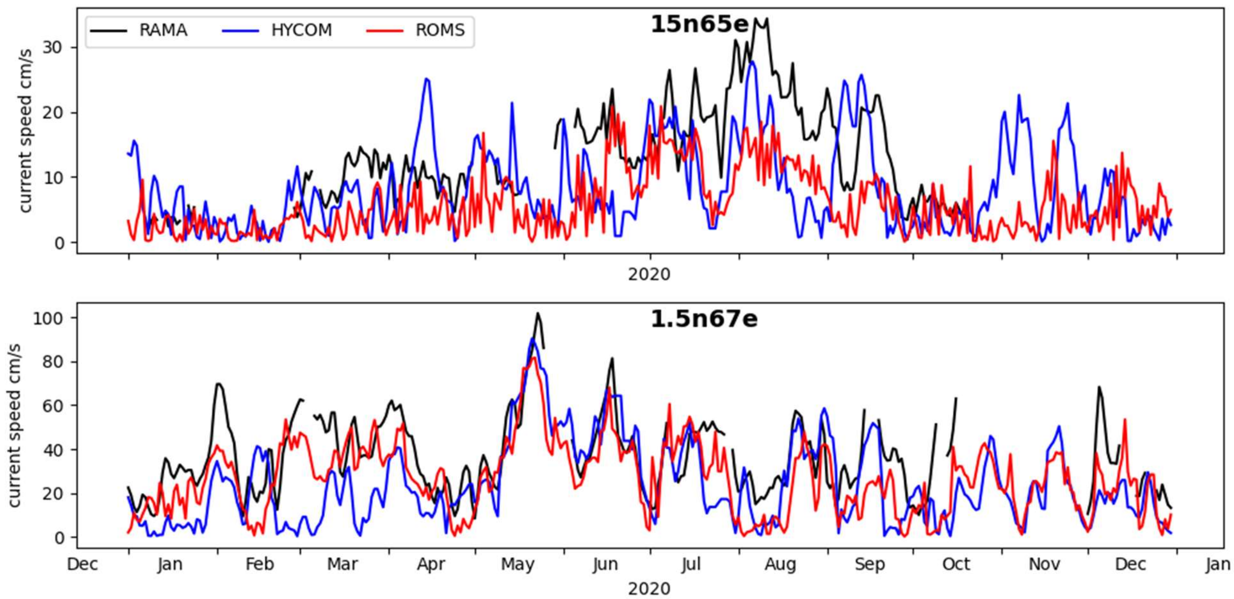

Figure 16: HYCOM and ROMS 1/12 Current Speed (cm/s) comparison at two RAMA locations

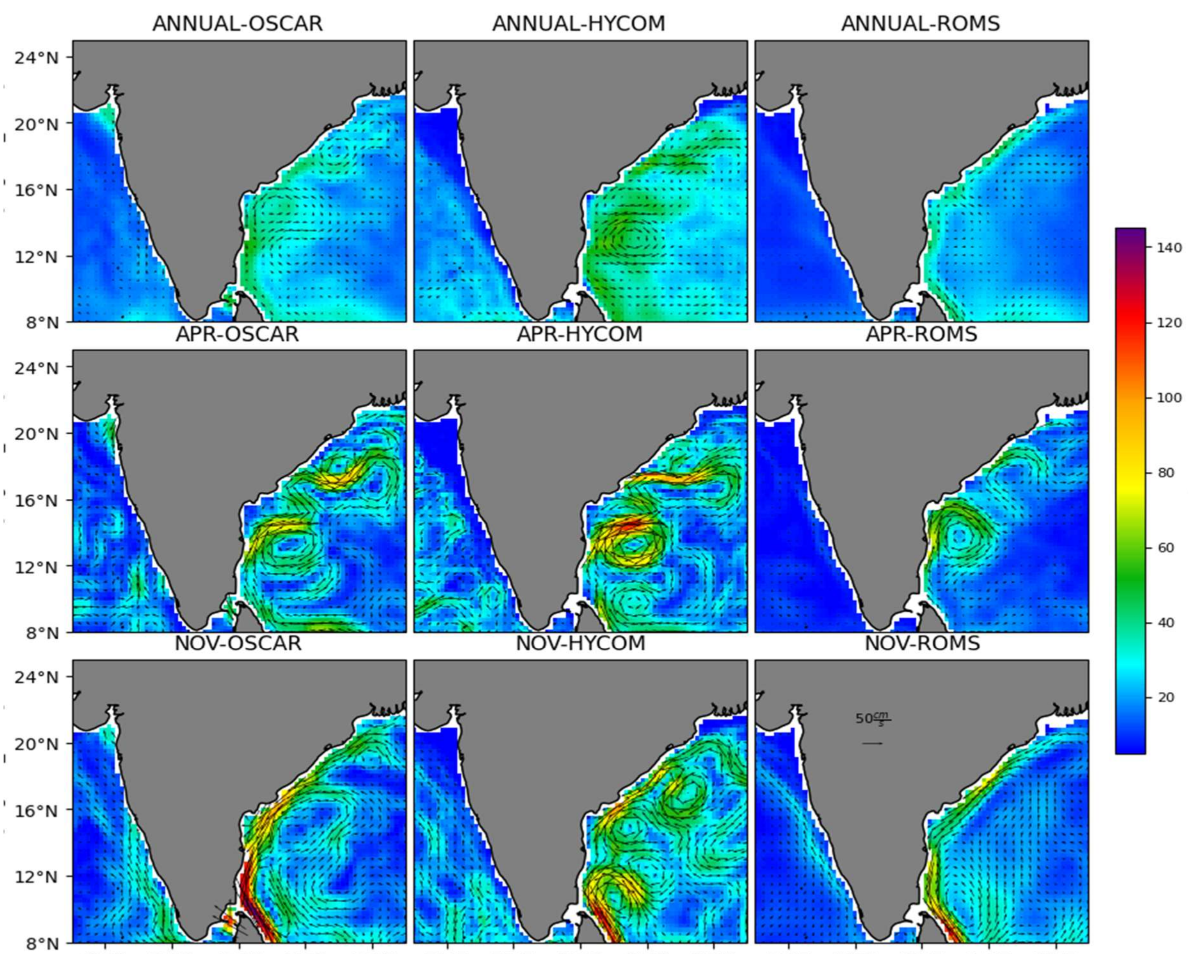

Figure 17:Spatial distribution of Current Speed (cm/s) and vector from OSCAR analysis (left panel), HYCOM (middle panels), and ROMS 1/12 (right panels) for Annual mean, April and Nov.

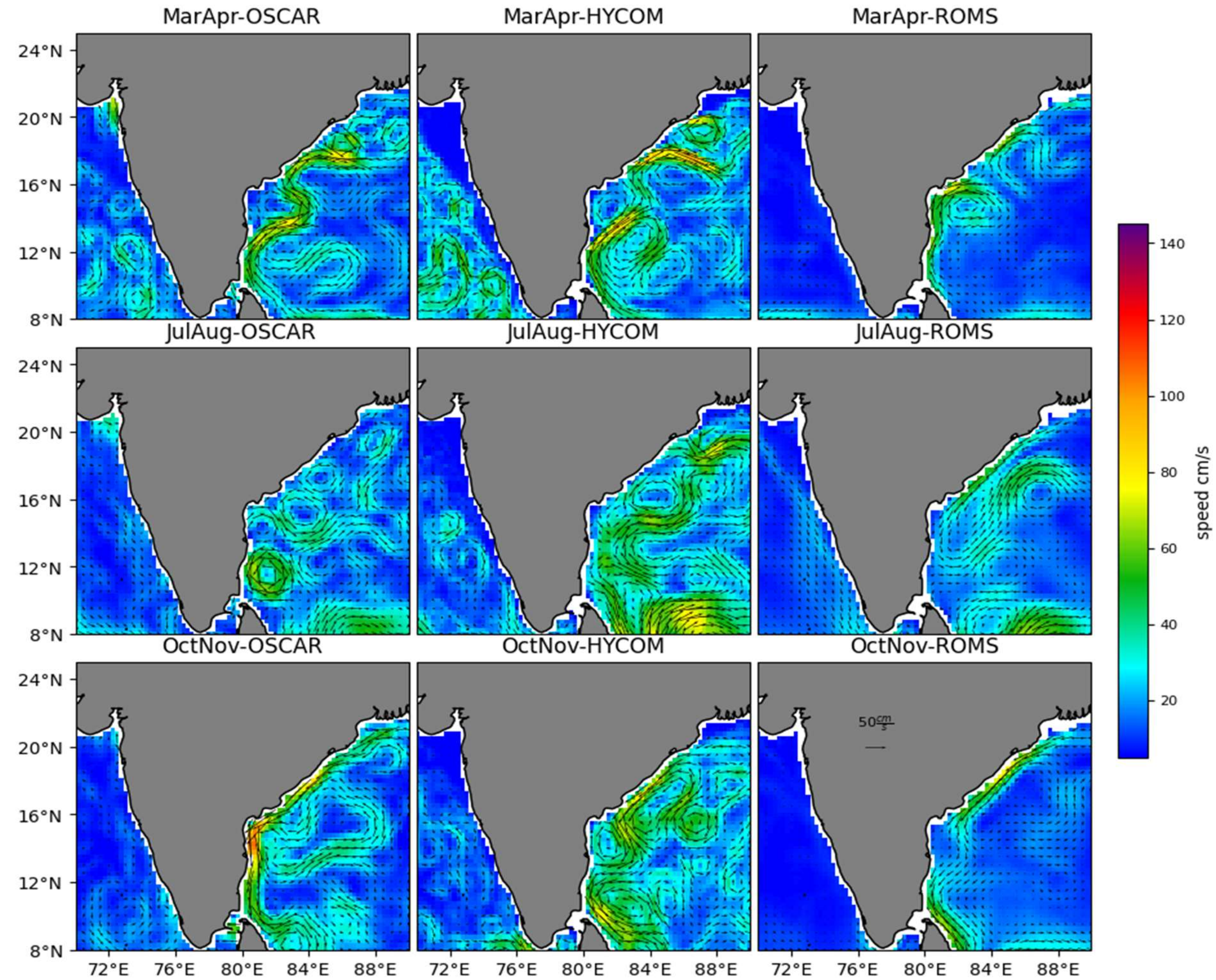

Figure 18: Same as figure 17 but for Mar-Apr (upper panels), Jul-Aug(middle panels), and Oct-Nov (lower panels).

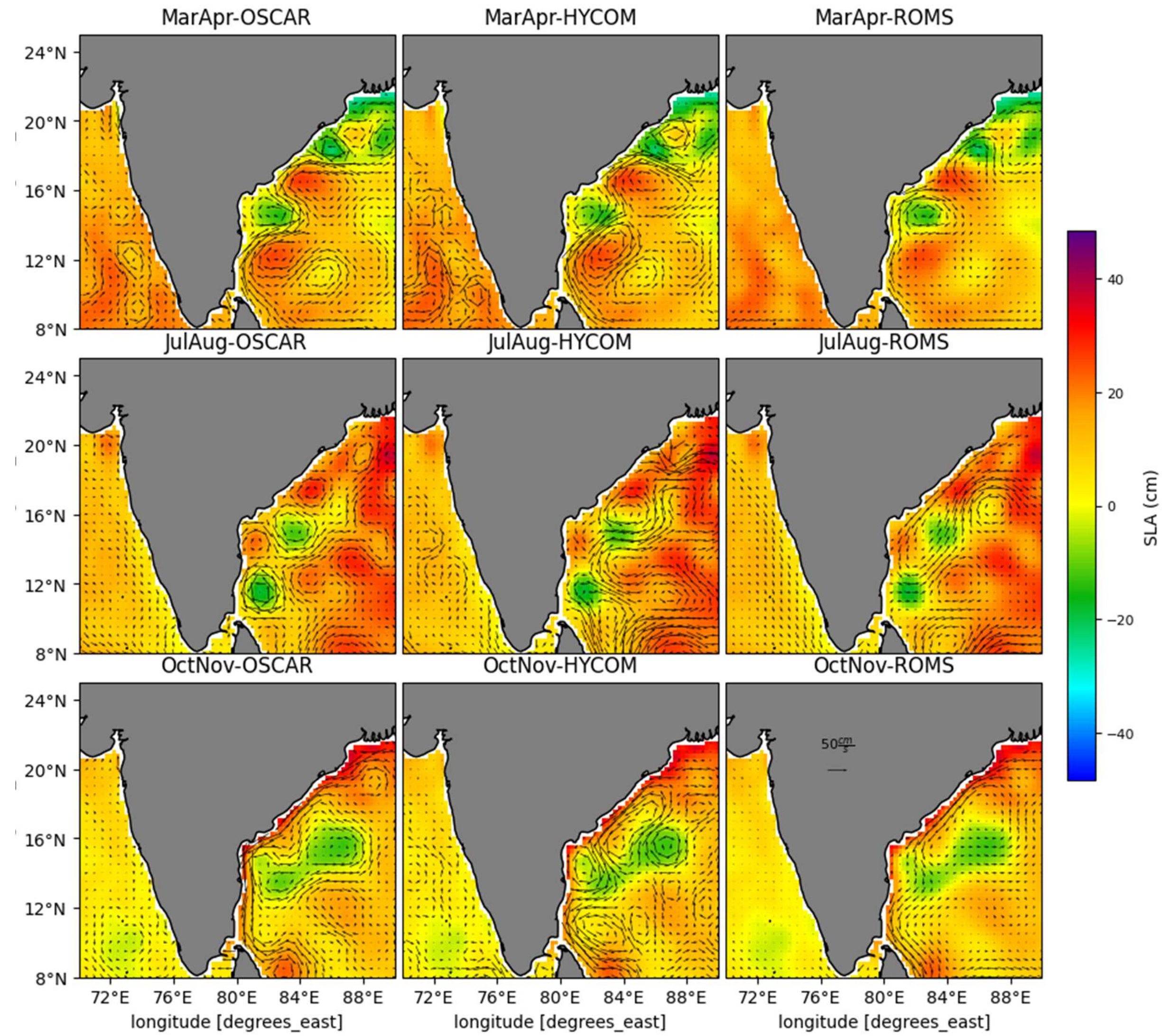

Figure 19: Currents vector plots are the same as Figure 18 but the shaded plots are for sea level anomaly(SLA) from AVISO observations for Mar-Apr (upper panels), Jul-Aug (middle panels), and Oct-Nov (lower panels).

5.3 Sub-surface current comparison with OMNI buoy observations

Figure 20 shows the subsurface comparison of HYCOM and ROMS current speed at 25 m, 50 m, and 100 m depth at the AD7 OMNI buoy location located in the southeastern Arabian Sea. It can be seen that both HYCOM and ROMS are unable to capture the buoy observed current speed at all these three depths. HYCOM performed slightly better as compared to ROMS in terms of daily variability. ROMS underestimates the buoy observations significantly. It significantly underestimates the daily variability at 100 m depth. At 25 m depth HYCOM on the other hand overestimates the observed current speed almost throughout the year except few sporadic events when its underestimates. A similar pattern was also observed for HYCOM at 50 m depth as well. At 100 m depth, HYCOM too underestimates the observed current speed except few events when it overestimates. However, ROMS current speed significantly underestimates the observed values at 100 m depth.   Over the northern BoB buoy location at BD08, a similar variation to that of AD7 was also observed (Figure 21).

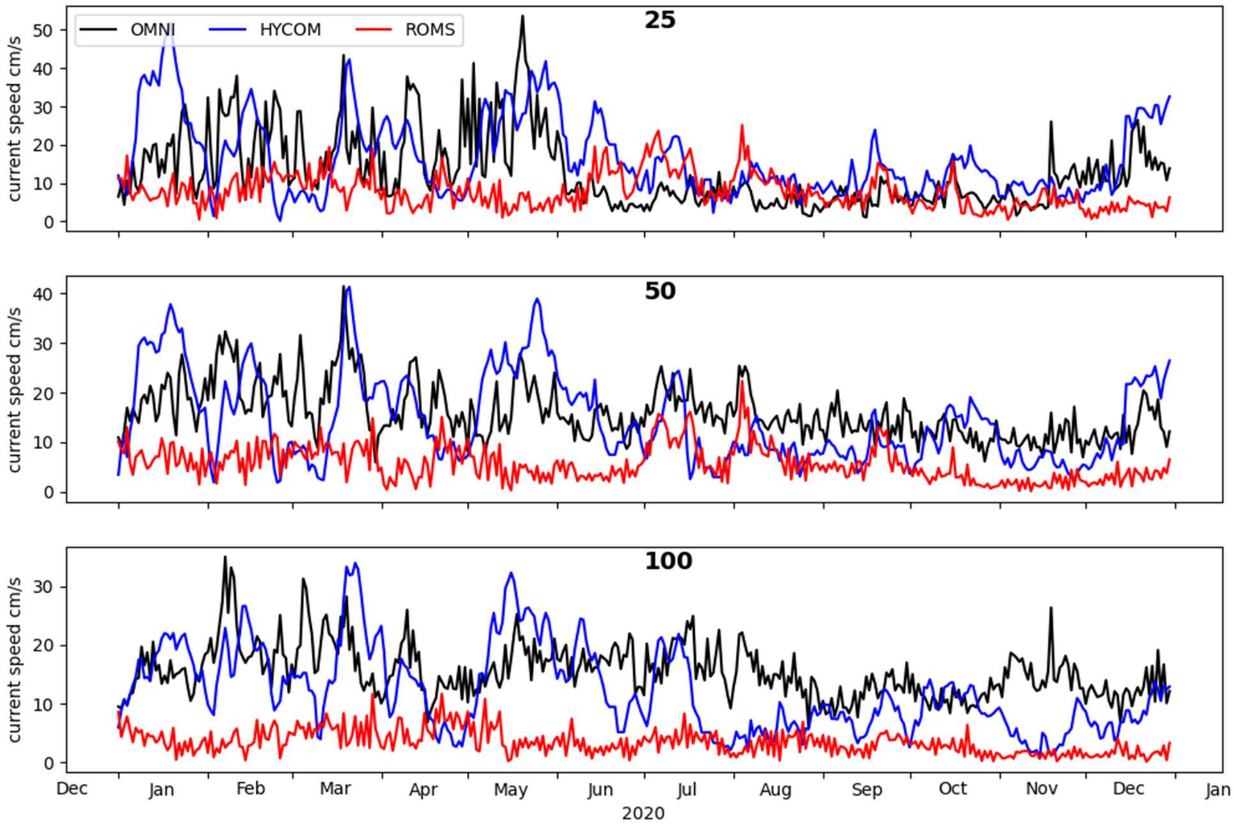

Figure 20: Time series comparisons of HYCOM and ROMS 1/12 Current Speed (cm/s) with ADCP observations at 25 m (upper panel), 50 m(middle panel and 100 m (lower panel) depths at AD07 buoy location(Arabian Sea).

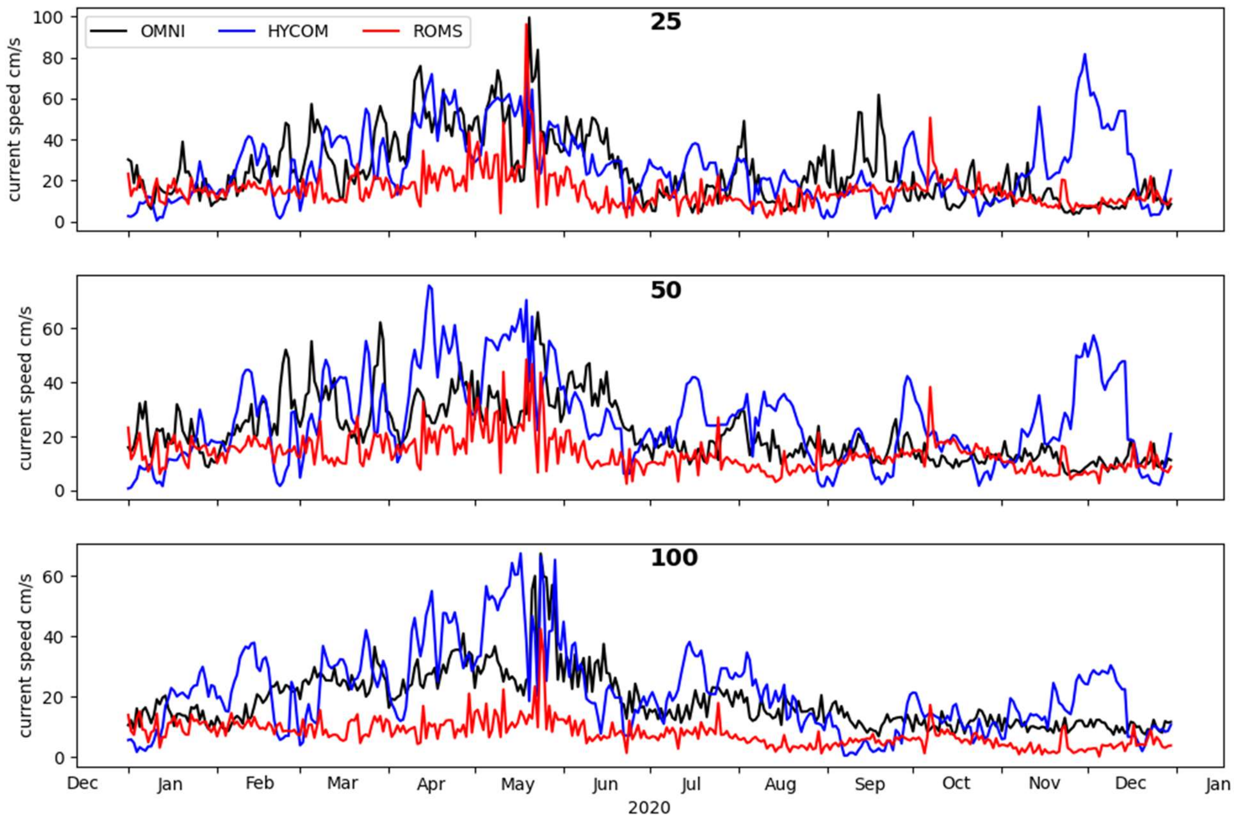

Figure 21: Same as Figure 20 but at BD08 buoy location(Bay of Bengal).

5.4 Costal current comparisons with HF-RADAR

High frequency (HF) radars, provide the total surface currents (Geostrophic + Ekman + Eddies + Tides) at high spatio-temporal resolution up to an offshore distance of about 200 km (Arunraj et al. 2018). The National Institute of Ocean Technology (NIOT), Ministry of Earth Sciences (MOES), Government of India has deployed a network of HF radars comprising 5 pairs of radar at the coasts of Andhra Pradesh, Tamil Nadu, Orissa, Andaman, and Gujarat and named as Indian Coastal Ocean Radar Network (ICORN).Its providing surface current since 2008 (Jena et al. 2019). Surface currents data from the Tamil Nadu coast for 1 year, from January 2020 to December 2020 have been used to evaluate the first-day current forecast of coastal currents from HYCOM and ROMS. Tamil Nadu coasts have two HF radar stations on the southeast coast of India, at Kalpakkam (80.15 °E, 12.49 °N) and at Cuddalore (79.77 °E, 11.68 °N). Figure 22 shows the annual, spring(Mar-April), and fall(Oct-Nov) current speed comparison. It can be seen that HYCOM slightly overestimates the current speed but is unable to capture the directions observed in HF radar. ROMS current is underestimated and also unable to capture the directions observed by HR radar. Both simulations are unable to capture the observed anticyclonic circulation seen in November very near the coast in fall (Oct-Nov).

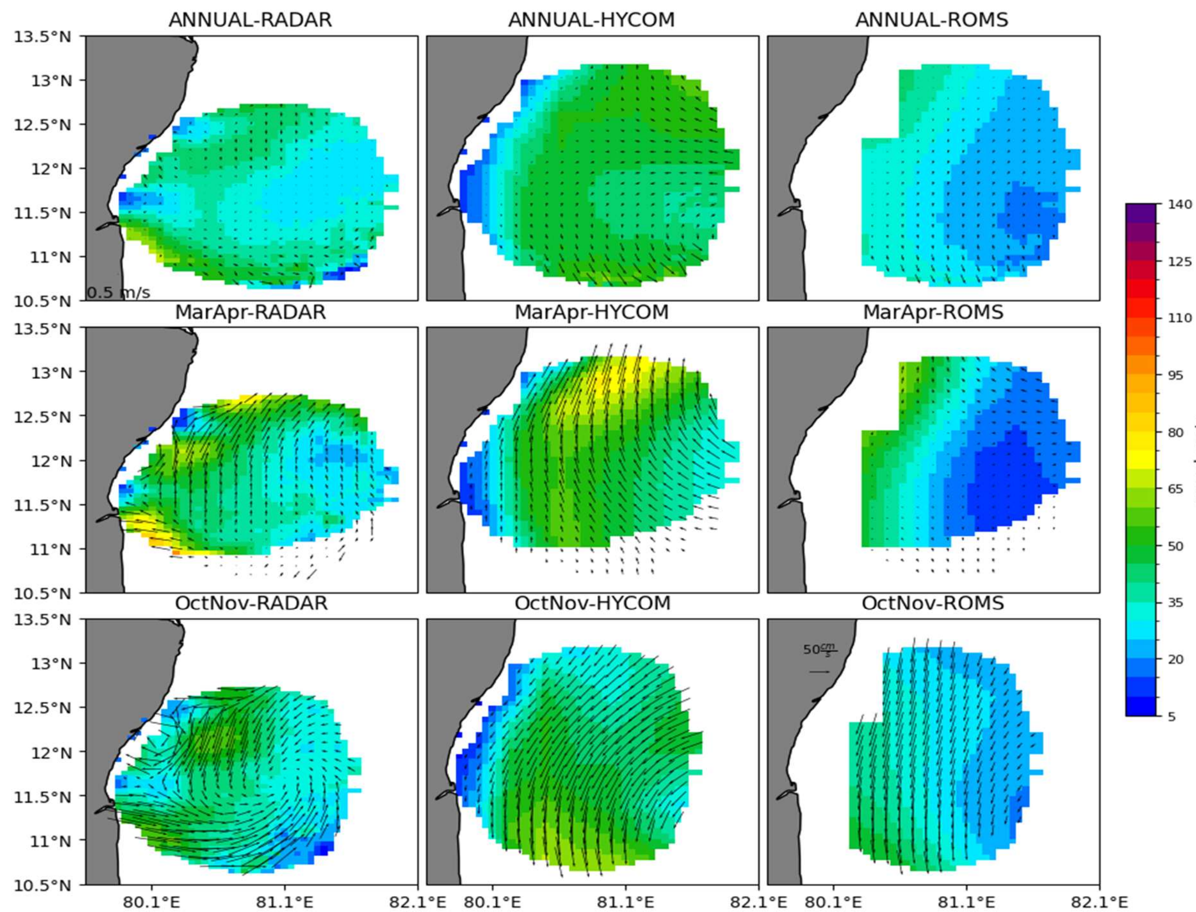

Figure 22: Annual (upper panels), Mar-Apr(middle panels), and Oct-Nov(lower panels) shows the HYCOM and ROMS 1/12 surface current speed (cm/s) and vector comparison with HF-Radar observations located off Tamil Nadu (TN) state of India. Model fields are masked with HF-Radar fields.

Figure 23 shows the correlation of first-day forecasted surface zonal, meridional current, and current speed of HYCOM and ROMS with HF radar observations. HYCOM meridional current CC values show high over most of the domain with maximum values of 0.85, over the same location its CC values are slightly lower for the zonal current. For the speed ROMS CC values (~ 0.4-0.6) are slightly higher than HYCOM (~ 0.2-0.5). The HF radar grid area-averaged surface zonal, meridional, and current speed comparisons are shown in Figure 24. Both HYCOM and ROMS are unable to capture the variability of observed HF current with HYCOM slightly better performed.

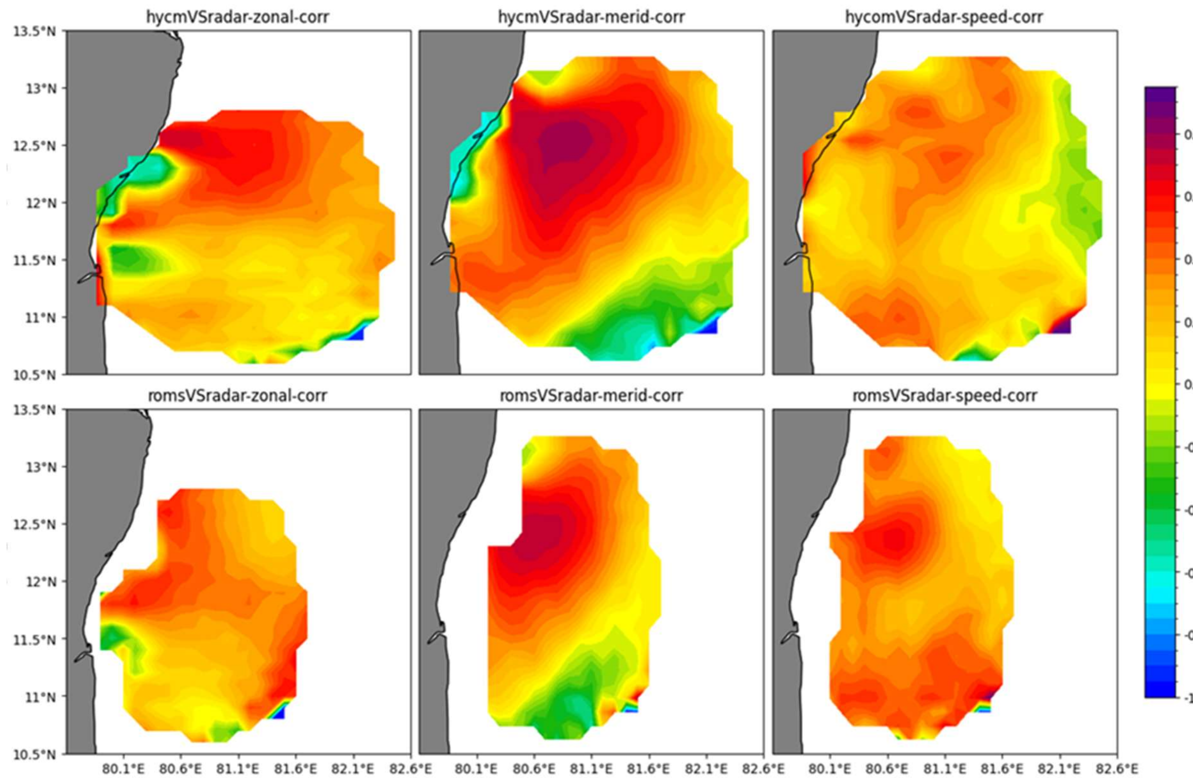

Figure 23: Spatial correlation of HYCOM and ROMS 1/12 surface current (cm/s) with HF-Radar observations located off Tamil Nadu (TN) state of India for zonal current (left panels), meridional current (middle panels) and current speed (right panels).

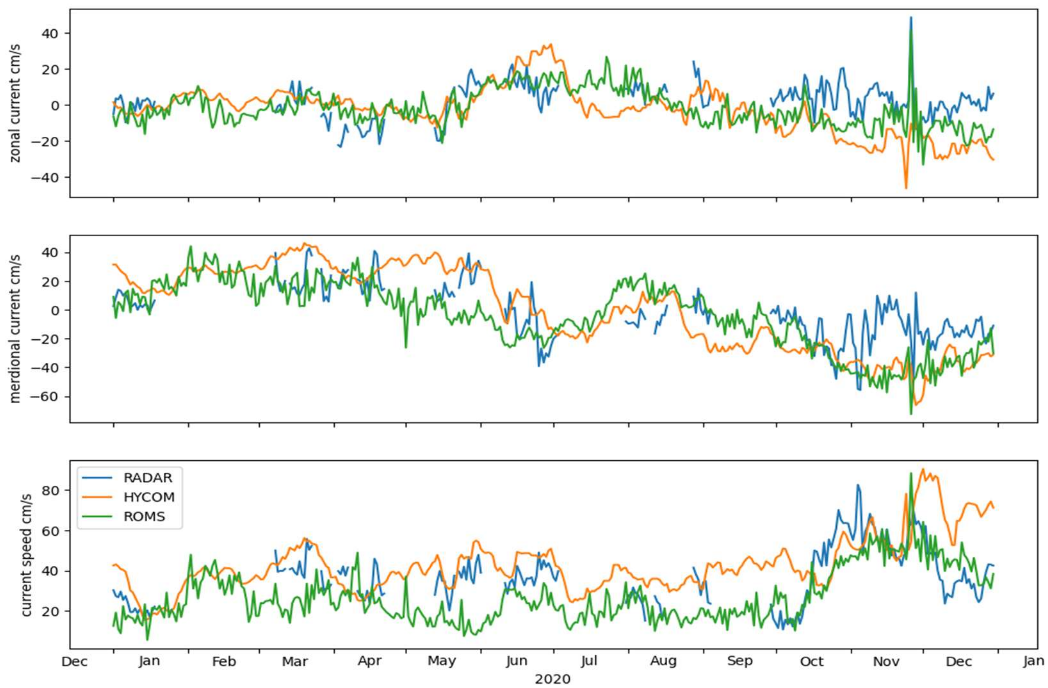

Figure 24: Time series comparisons of spatial averaged HYCOM and ROMS 1/12 surface current (cm/s) with HF-Radar observations located off Tamil Nadu (TN) state of India for zonal current (upper panel), meridional current (middle panel) and current speed (lower panel).

5.5 Impact of model resolution on forecast (ROMS 1/12 vs ROMS 1/48)

In this section, we show the impact of model resolution on SST and current forecasts over the Bay of Bengal and along the coast of India. First-day SST forecast RMSE significantly reduced near the coast in ROMS 1/48 degree as compared to 1/12 degree (Figure 25).

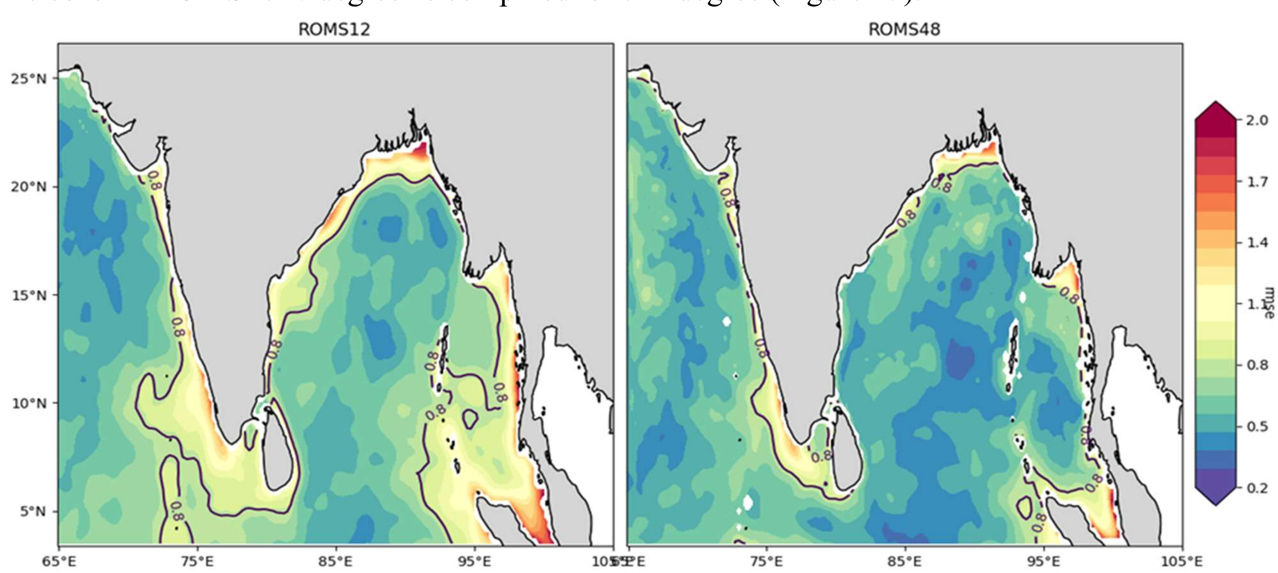

Figure 25: Spatial SST RMSE (°C) of ROMS1/12 and ROMS1/48 with respect to NOAA OI SST.

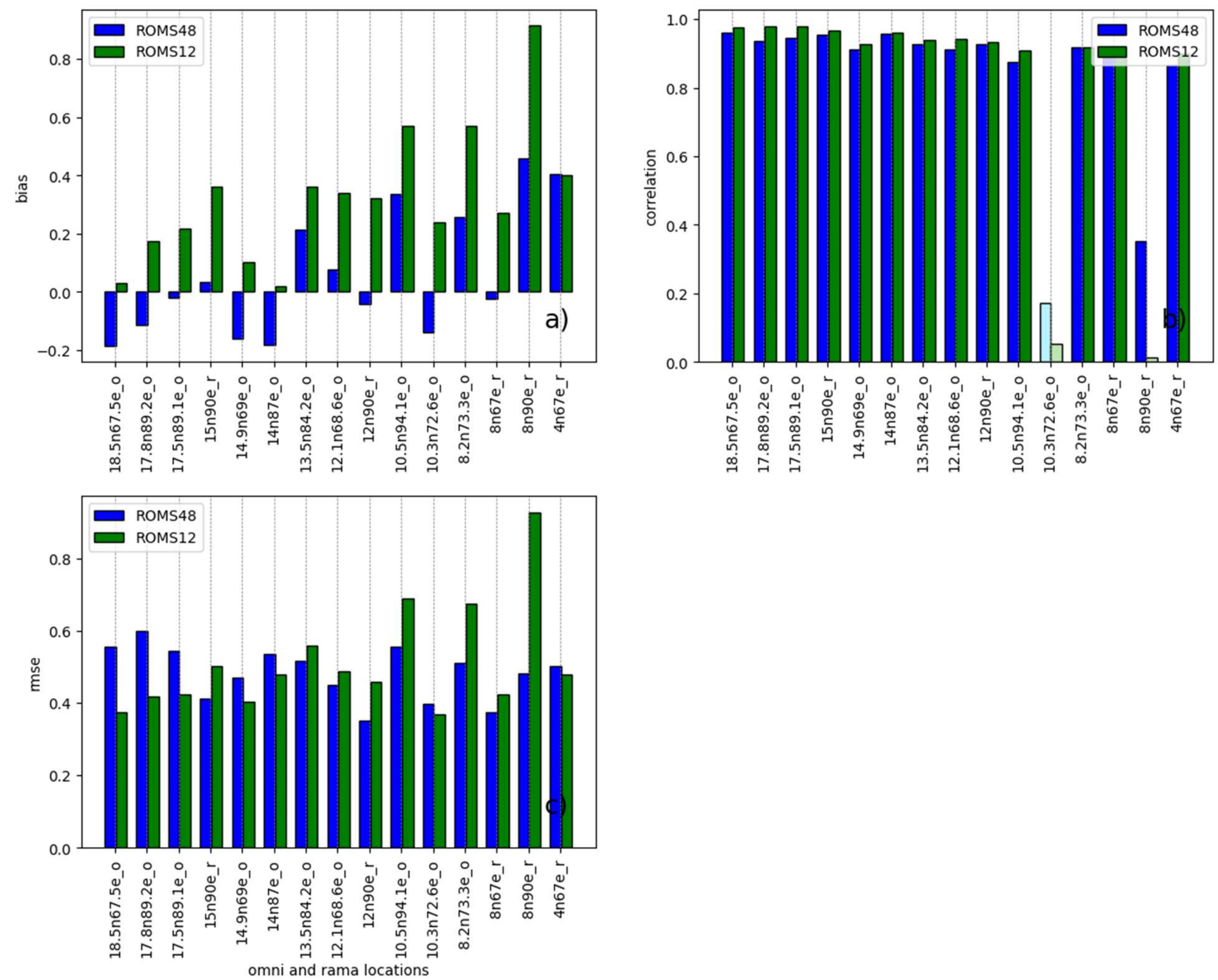

Figure 26: *Location-wise statistics plots of SST with respect to OMNI and RAMA buoy observations (a)bias (°C), (b) correlation coefficient, and (c) RMSE (°C). All the metrics are for the year 2020 and the first-day forecast of ROMS 1/12 and ROMS 1/48.*

Comparison with OMNI and RAMA buoy shows a significant reduction of bias in 1/48 as compared to the 1/12 forecast (Figure 26a). However, except for a few buoy locations, in all other buoy locations, the CC values show higher in 1/12 as compared to 1/48 degrees (Figure 26b). It is worth mentioning that CC values are very low at 10.3 °N and 72.6 °E OMNI buoy location for both ROMS 1/12 and ROMS 1/48. This could be due to a very low number of co-located points (See Table 1). Similarly, for the RMSE too except for a few buoy locations all other locations show higher values in ROMS 1/48 as compared to ROMS 1/12 (Figure 26c). The skill score computed with reference to three different reference forecasts described in sec 5.1 form ROMS 1/12 and ROMS 1/48 are shown in Figure 27. It can be seen that SS values are lower in ROMS 1/48 as compared to ROMS 1/12. The SS based on buoy climatology as a reference forecast shows negative skill in most of the locations for both ROMS 1/12 and 1/48 except few locations where ROMS 1/12 shows positive SS values (Figure 27a). ROMS 1/12 SST SS values show positive values at 18.5 °N,67.5 °E, 17.8°N,89.2 °E and 17.5 °N 89.1 °E. SS values over these three locations in

ROMS 1/48 are lower than ROMS 1/12, SS values even become negative at 18.5 °N, 67.5 °E (Figure 27a). The last two locations are in northern BoB. SS values based on NOAA-OI climatology as a reference forecast show positive SS values for all buoy locations for both ROMS 1/12 and 1/48 (Figure 27c). With enhanced resolution, the SS values in most of the buoy locations do not improve, in a few locations it's even degraded.

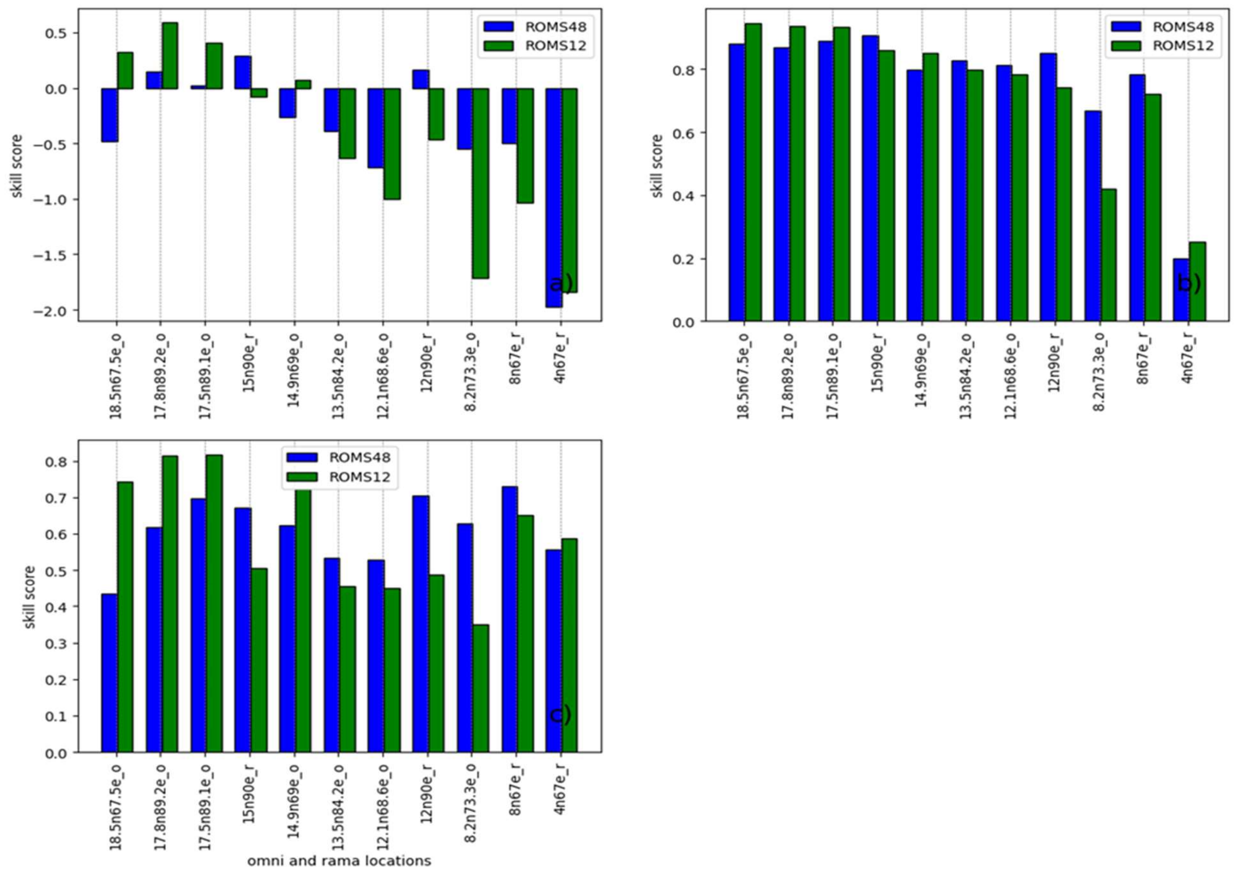

Figure 27: SST skill scores computed using different reference forecasts (a) observational climatology (b) observational standard deviation and (c) NOAA OISST as reference forecast for ROMS1/12 and ROMS1/48.

The spatial CC distribution of zonal, meridional, and current speed computed with respect to daily OSCAR analysis are shown in Figure 28. It can be seen that the CC value in zonal current shows degradation in ROMS 1/48 as compared to ROMS 1/12 (Figure 28). CC in meridional current does not show any major change. The effect of degraded zonal current CC values is reflected in current speed CC values shown in the lower bottom panel. The SS computed at 10 buoy locations over the BoB are shown in Figure 29. The skill score values too show degradation in ROMS 1/48 as compared to 1/12 (Figure 29). The SS value for ROMS 1/48 even becomes negative at 12.1 °N, 68.6 °E. However, its positive in ROMS 1/12. The daily time series comparison of surface current from OMNI buoy locations at BD14 at BoB (Figure 30) and AD07 at AS (Figure 31) shows both the model forecasts are unable to capture the observed variations. It even degrades in ROMS 1/48 as compared to 1/12. The spatial surface currents comparison during inter-monsoon and monsoon seasons with OSCAR analysis are shown in Figure 32. It shows ROMS 1/48 current speed magnitude enhanced but it overestimated the OSCAR analysis as compared to ROMS 1/12 which underestimates. The presence of spurious eddies can also be seen in ROMS 1/48 forecasted current when compared with OSCAR analysis. In conclusion, with enhanced resolution on the first day, the SST forecast degrades. Similar results can be found for the surface current forecast as well. This study further confirms the finding of Hyder et al. (2012) which shows no skill enhancement on hindcast surface current in the high resolution (1/12°) regional model compared to the coarser resolution (1/4°) global model over the Indian Ocean.

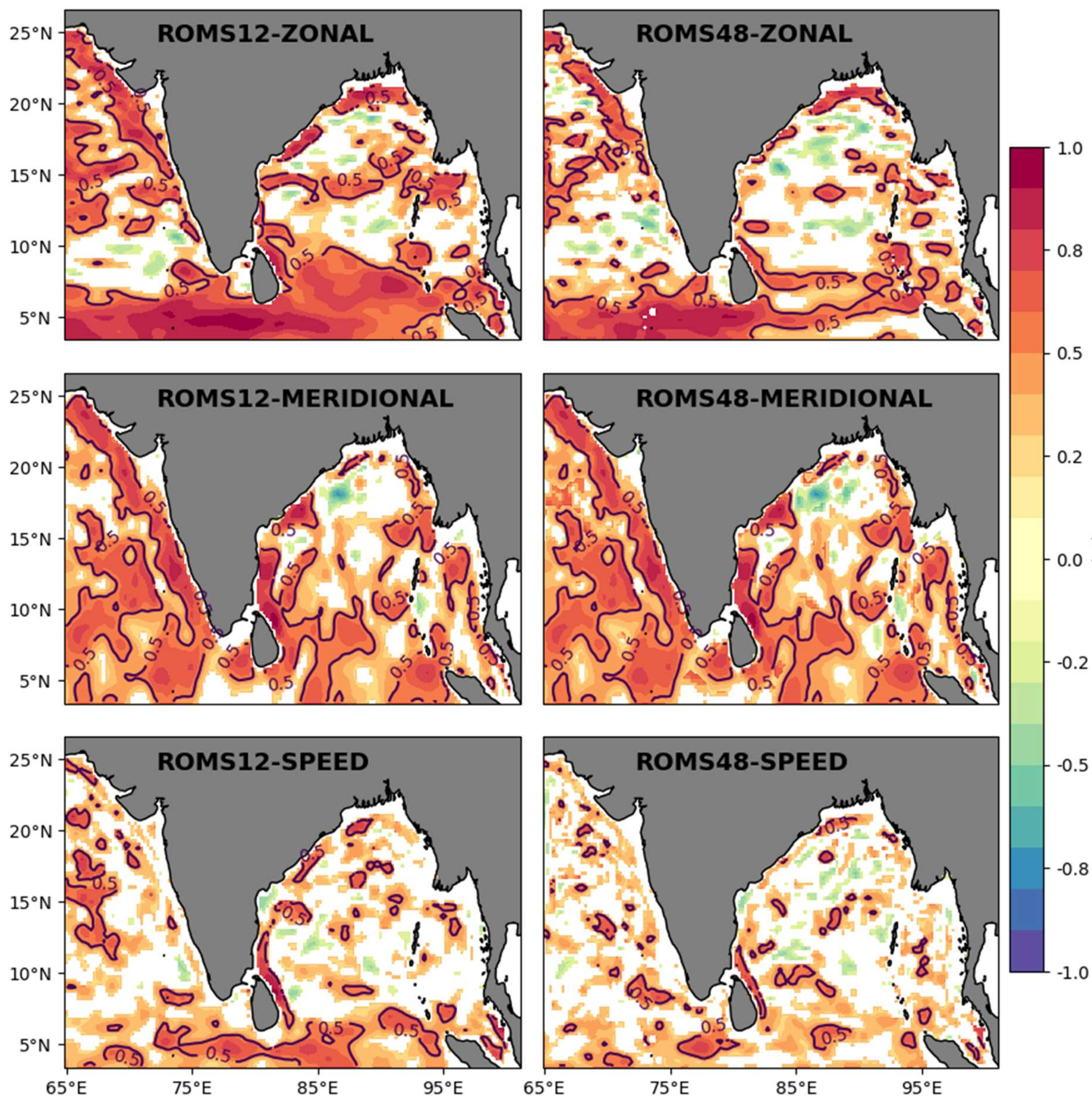

Figure 28: Correlations of zonal current (upper panels), meridional currents (middle panels), and current speeds (lower panels) of ROMS1/12 and ROMS1/48 with respect to OSCAR analysis.

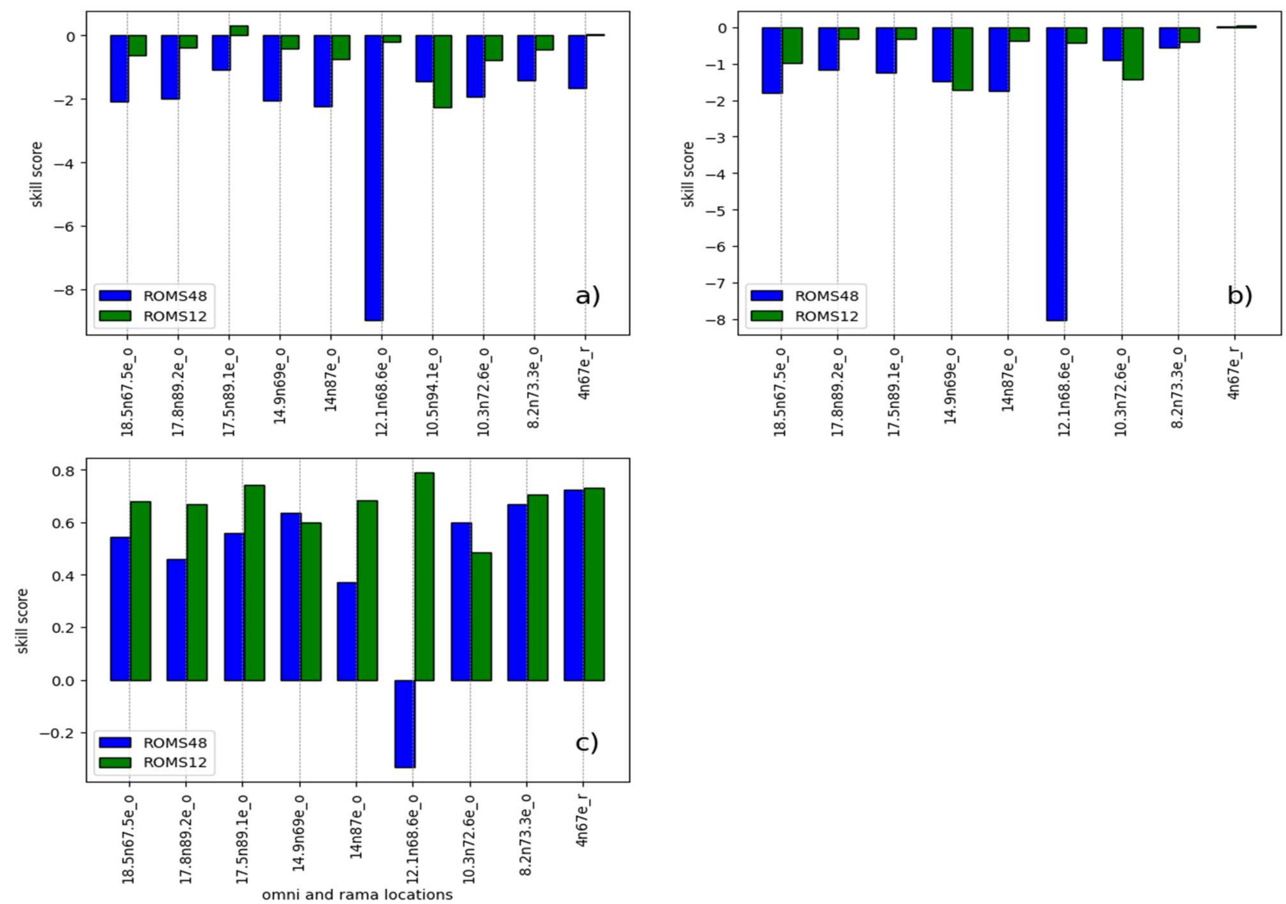

Figure 29: Comparison of ROMS 1/12 and ROMS 1/48 current speed skill scores computed with (a) climatological current speed (b) standard deviations and (c) OSCAR daily climatology as reference forecasts.

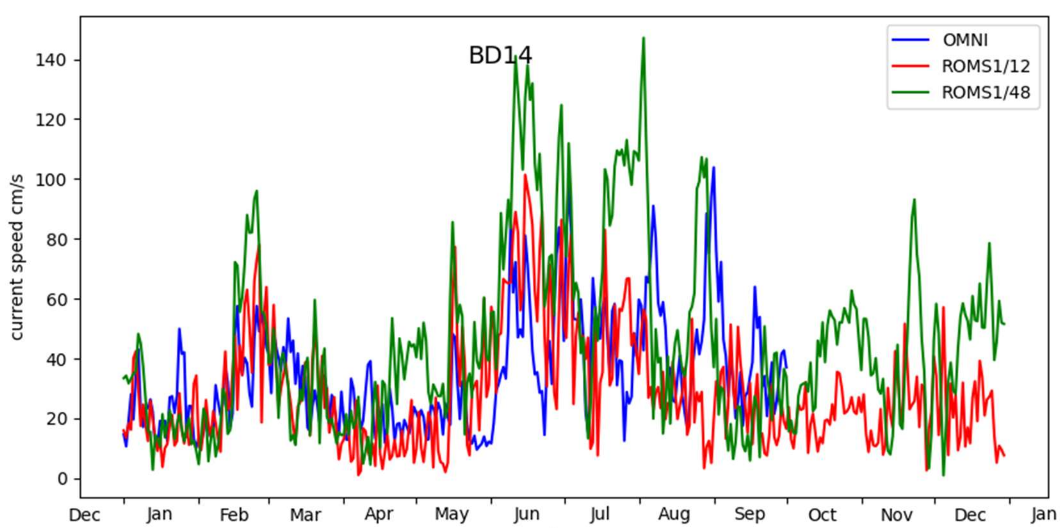

Figure 30: Time series comparison of surface current (15 m depth) from ROMS 1/12 and 1/48 with OMNI buoy observation at BD14 location (Bay of Bengal).

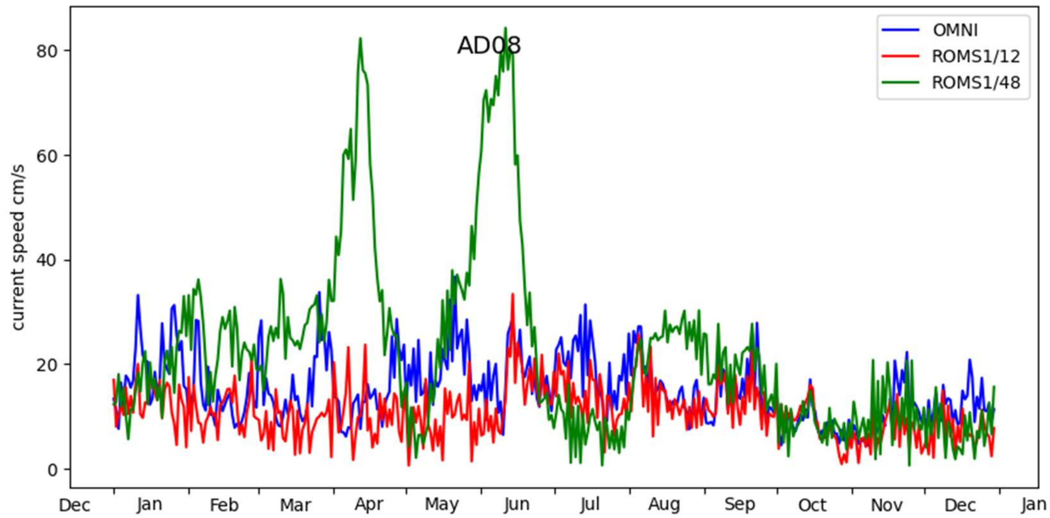

Figure 31: Time series comparison of surface current (15 m depth) from ROMS 1/12 and 1/48 with OMNI buoy observation at AD08 location (Arabian Sea).

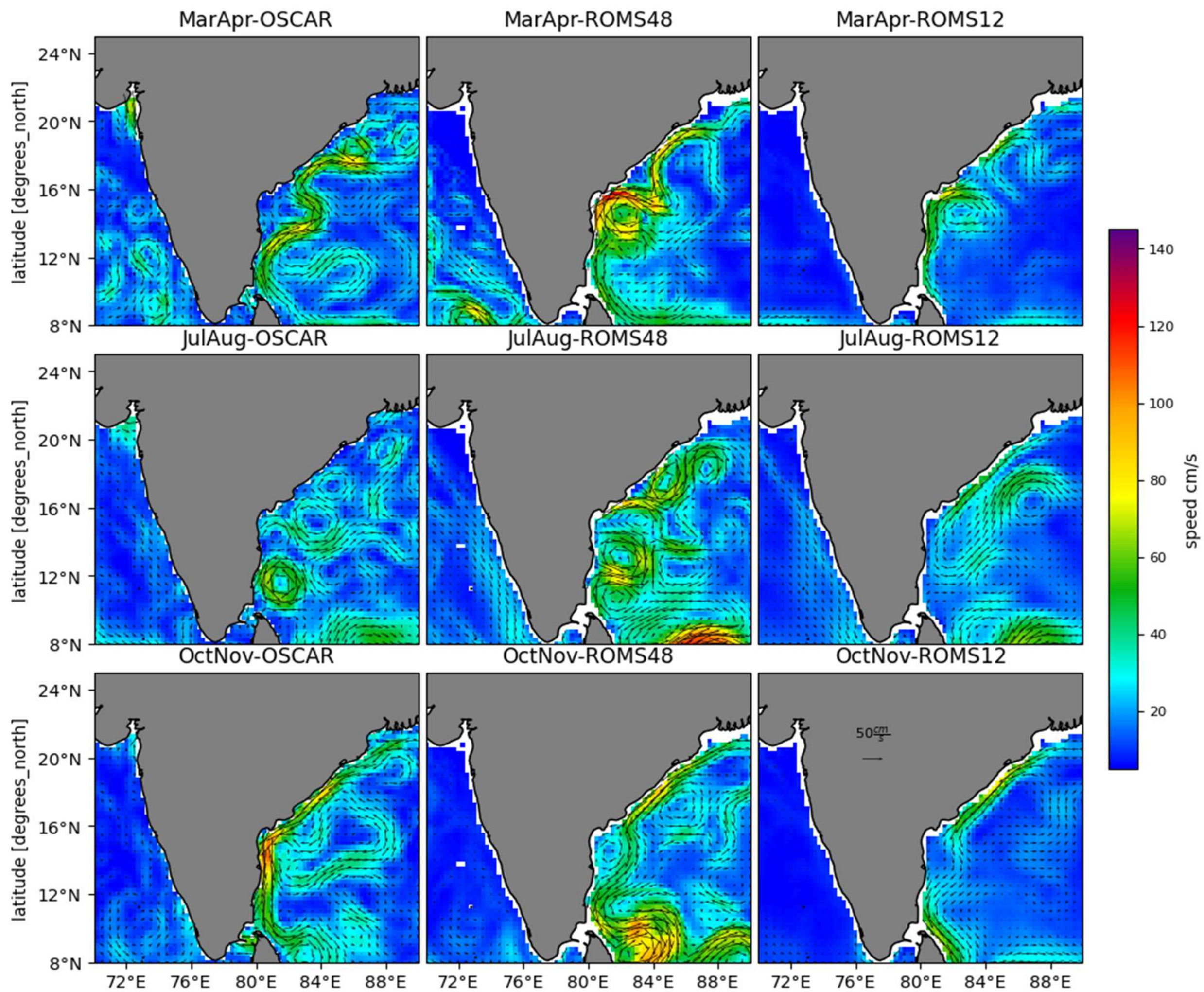

Figure 32: Current speed (cm/s) and vector comparisons of ROMS 1/12 and ROMS 1/48 for Mar-Apr (upper panels), Jul-Aug (middle panels), and Oct-Nov (lower panels).

5.6 Thermocline depth (D20) and mixed layer depth (MLD)

The mixed layer depth (MLD) plays a key role in determining the vertical distribution of many physical and ecological parameters. The thermocline is a physical gradient that plays a key role in climate variability and ocean-atmosphere interactions. The thermocline strength affects buoyancy, heat budgets, circulation, and exchange of properties and impacts Indian Summer Monsoon Rainfall (ISMR) inter-annual variability. Its depth is associated with the habitat and abundance of zooplankton organisms and is also an ecological boundary for pelagic organisms. Strong temperature changes can set habitat distributions, and the thermocline often corresponds to gradients in nutrients (nutricline), oxygen (oxycline), or other limiting factors. The thermocline thickness also affects the intensity of the primary production (Helber et al. 2008). In equatorial and tropical regions, the strong thermocline prevents nutrient-rich water from the deep layer from reaching the surface (Webb, 2021). The global variability of MLD is important to a wide variety of phenomena from tropical cyclone formation (Mao et al., 2000), to phytoplankton bloom critical depth theory (Siegel et al., 2002), to climate variability (Deser et al., 2003). Numerical prediction of MLD is challenging in that the vertical structure of the temperature and salinity model fields tends to be overly smooth, resulting in a shallow bias (Kara and Hurlburt, 2006). Sonic layer depth (SLD) plays an important role in antisubmarine warfare in terms of identifying the shadow zones for submarine safe parking. SLD is estimated from sound velocity profiles (SVP) which in turn is obtained from temperature and salinity (T/S) profiles. Often the SLD and the MLD coincide because the sound speed is locally maximum at the base of the isothermal and/or isohaline surface layer. Hence, accurate prediction of MLD variability will help the navy to strengthen national security.

The AS hosts one of the most pronounced oxygen minimum zones (OMZs) among all the oceans in the world. The presence of low-oxygen water in the subsurface layer affects marine habitat and, thus, a large coastal population that depends on marine fisheries for their food and economy. It is, therefore important to understand the dynamics of OMZ. Prakash et al. (2013) have shown that the variability in oxycline depth is governed by the variability in the thermocline depth, i.e. the shallowing of the thermocline is associated with the corresponding shallowing in the oxycline and vice versa. Hence, the depth of the thermocline forecast over the Indian Ocean, particularly over the Bay of Bengal and the eastern Arabian Sea has immense importance for the PFZ advisory INCOIS provides to the fisherman community. Apart from these two important ocean parameters, the thermocline depth in the ocean as well as the Tropical Cyclone Heat Potential (TCHP) are responsible for the genesis, intensification, and propagation of tropical cyclones. Hence, accurate MLD and D20 prediction will be very useful for Cyclone prediction.

In this section, we discussed the first day D20 and MLD forecast from INCOIS operational models. Figure 33 shows the comparison of the spatial distribution of 1st day D20 forecast from ROMS and HYCOM with gridded ARGO observations. It can be seen that the HYCOM D20 forecast shows a closer match with the observed distribution as compared to ROMS over the entire Indian Ocean basin. ROMS shows deeper D20 as compared to HYCOM and Argo observations. The observed D20 over BoB shows ~ 110-130 m which is deeper in ROMS 1/12 forecast ~ 140-160 m (Figure 34).. This deeper D20 becomes shallower in the ROMS 1/48 forecast and matches well with the Argo observed pattern. However, HYCOM shows most closest to the Argo observation. Biases in ROMS 1/48 D20 forecast over the BoB reduced considerably as compared to its coarse resolution 1/12 degree products but still its under-performs HYCOM which is close to the observations (Figure 35).

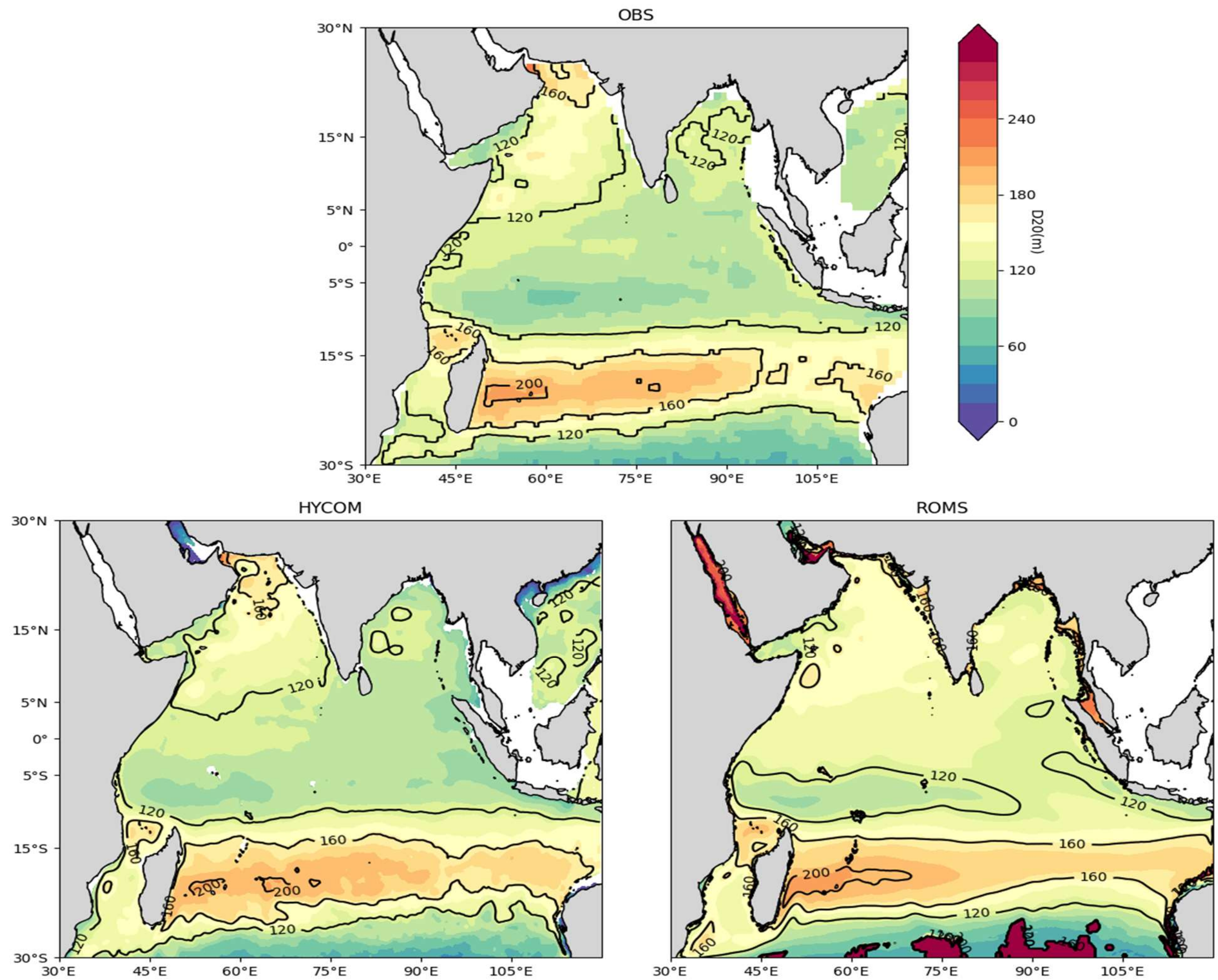

Figure 33: Annual mean spatial D20 (m) from Argo observation (upper panel), HYCOM (lower right panel) ROMS 1/12 (lower right panel).

The seasonal cycle of D20 averaged over different regions given in Figure 2 is shown in Figure 36. Both ROMS and HYCOM could able to capture the observed seasonal cycle. Over almost all regions, ROMS D20 is deeper than Argo observations. HYCOM forecast is relatively close to the observed seasonal cycle as compared to ROMS. HYCOM almost reproduced the observed seasonal cycle over the western and eastern equatorial Indian Ocean. HYCOM could reproduce the seasonal cycle over the BoB but shows a systematic shallower (~ 10 m) D20 with respect to Argo observation. ROMS shows a much deeper D20 over the SIO region from June to November. This could be due to the boundary issue since this region is very close to the southern boundary of the model domain and spatial plots also show similar deeper D20 over this region (Figure 33). We also compared the D20 with OMNI and RAMA buoy observations. The bias, CC, and RMSE for ROMS and HYCOM at 12 RAMA and OMNI buoy locations are shown in Figure 37. Similar to the Argo observation comparison, buoy observations also show ROMS D20 is much deeper and ranges ~ 5 to 22 m in different buoy locations. On the other hand following the similar results to that of Figure 36, HYCOM D20 shows a shallower over most of the buoy locations ranging ~ -2 to -14 m, except two buoy locations at 65 E where it shows deeper D20 ~ 6 to 10 m as compared to the buoy. CC values are also high in HYCOM as compared to ROMS in most of the buoy locations. RMSE values are also lower in HYCOM ~ 5 to 20 m as compared to ROMS ~ 8 to 28 m (see Tables 7 and 8). Daily observed D20 variability is also very well captured in HYCOM as compared to ROMS (See Tables 7 and 8). Enhanced resolution degrades the D20 forecast as CC (RMSE) values show lower (higher) in ROMS 1/48 as compared to ROMS1/12 (see Figure 38).

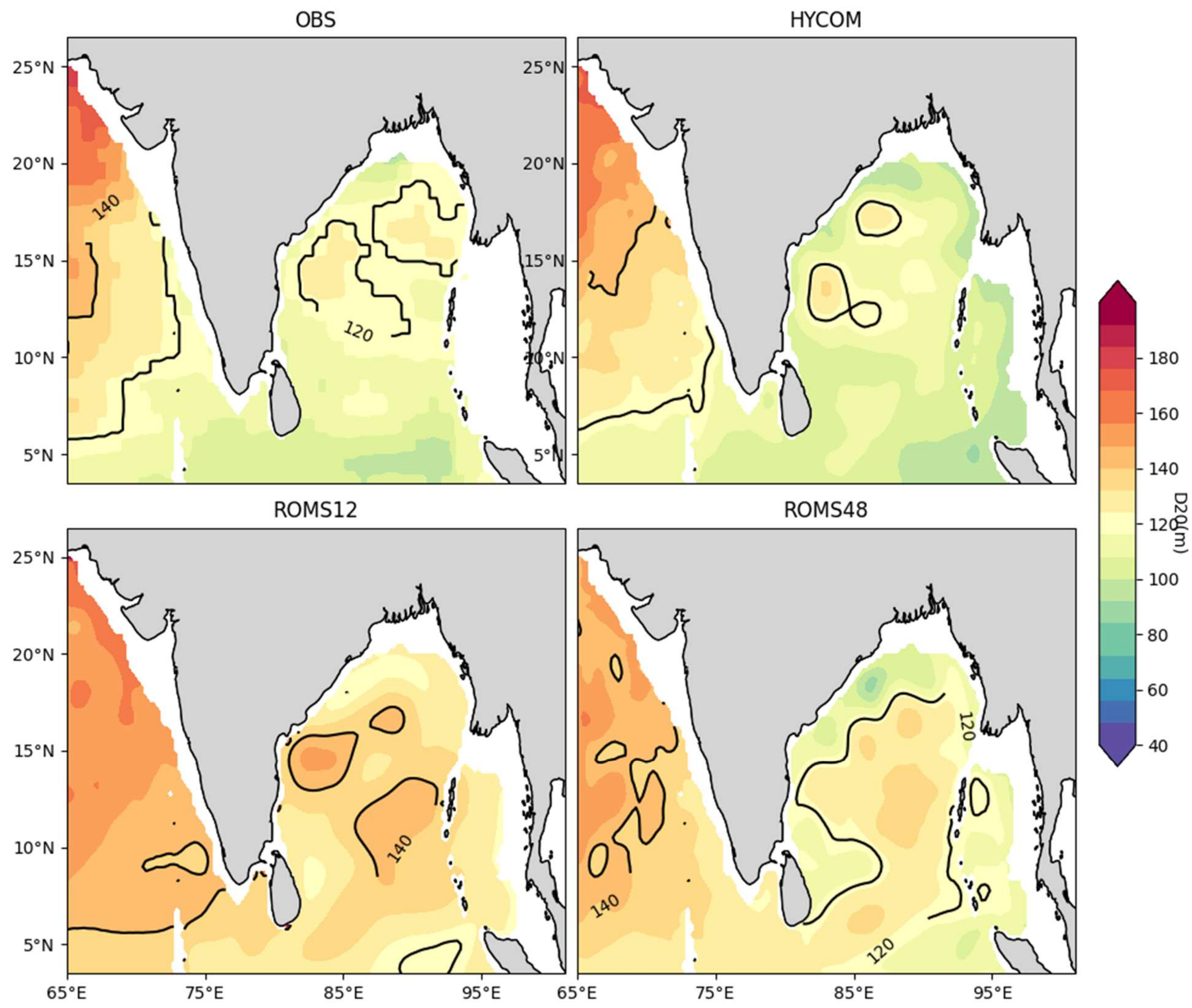

Figure 34: Same as Figure 33 but over the Bay of Bengal which includes ROMS 1/48 as well.

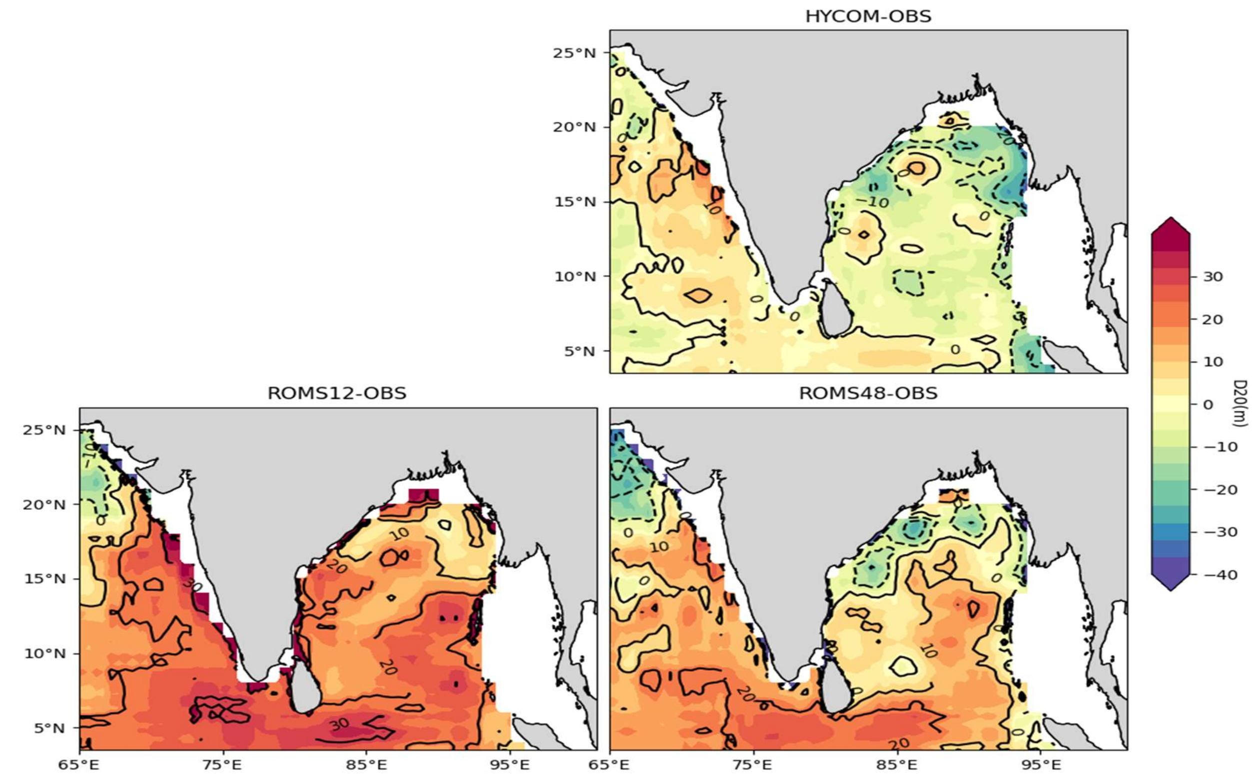

Figure 35: Annual mean spatial bias of D20 (m) over the BoB.

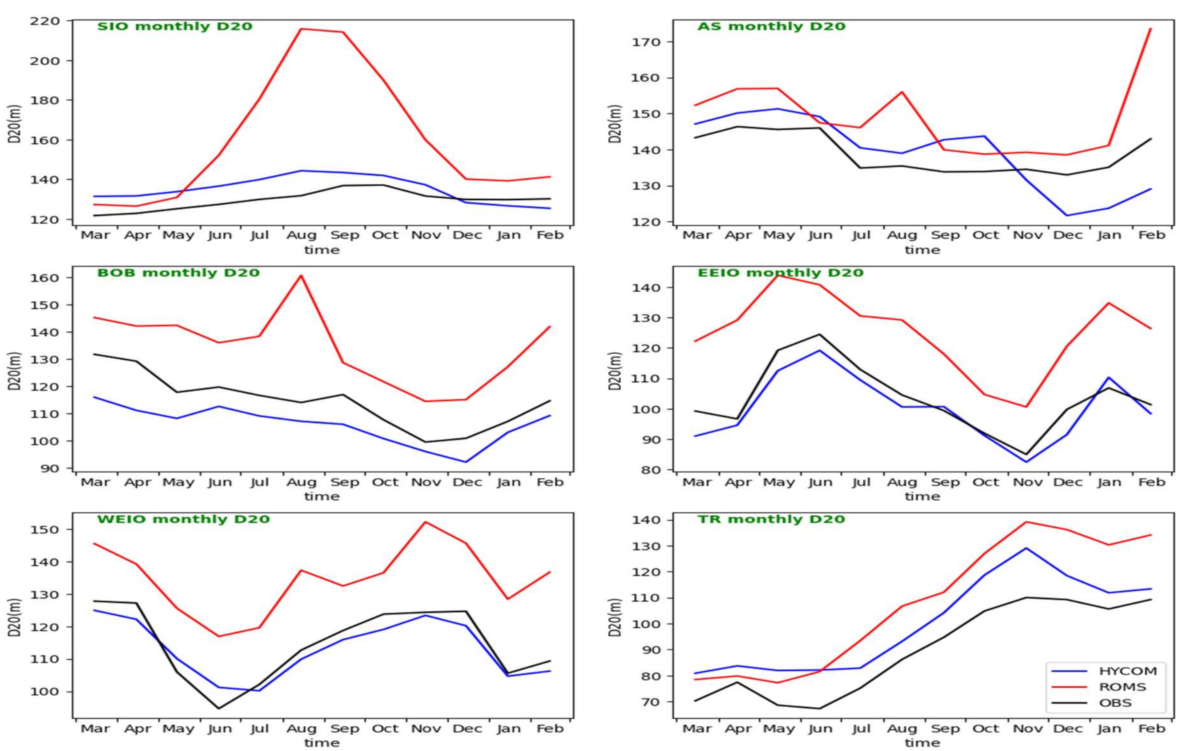

Figure 36: D20 seasonal cycle averaged over different regions defined in Figure 1b.

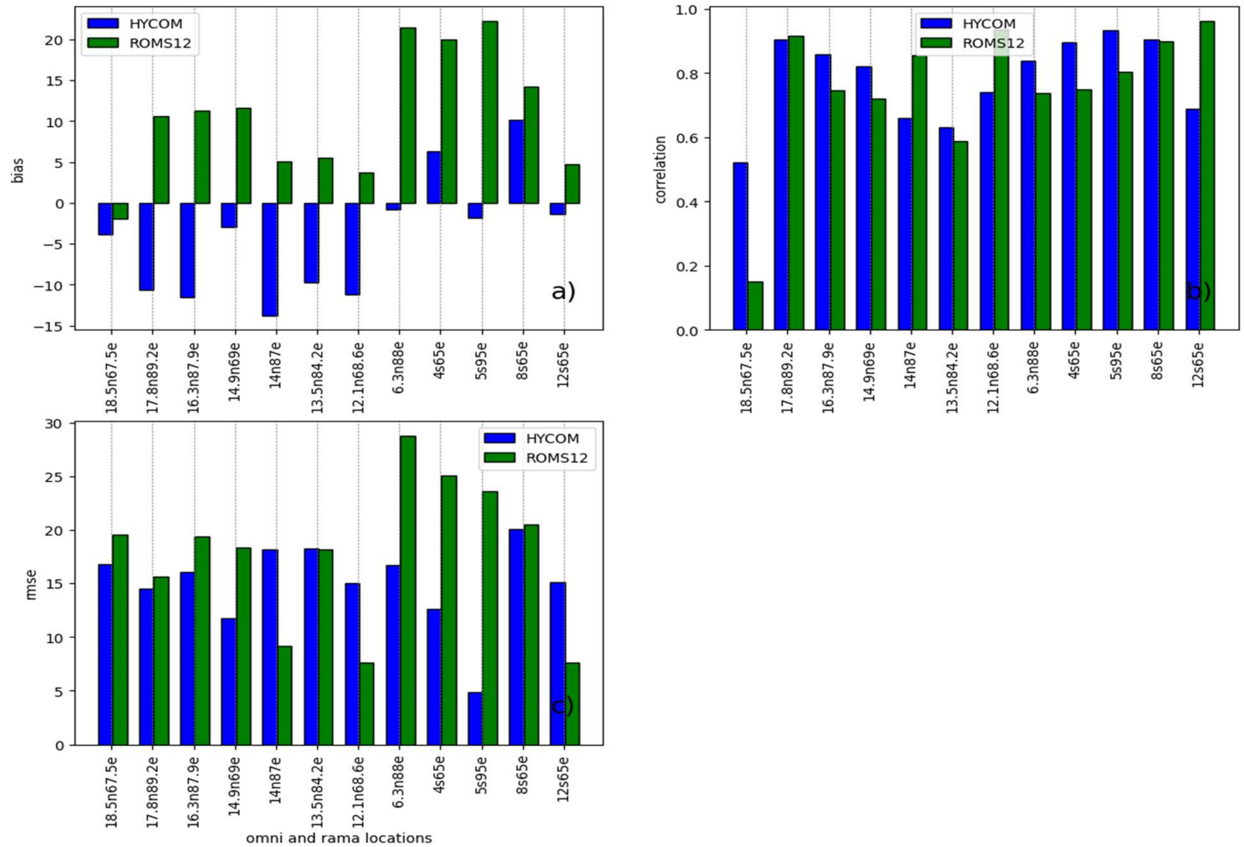

Figure 37: Location-wise statistics plots of HYCOM and ROMS 1/12 D20 with respect to OMNI and RAMA buoy observations (a)bias (m), (b) correlation coefficient, and (c) RMSE (m).

Table 7. D20 statistics of HYCOM and ROMS at OMNI buoy locations

	BIAS (m)		CORR		RMSE (m)		STD (m)			VALID POINTS
Buoy	HYCOM	ROMS	HYCOM	ROMS	HYCOM	ROMS	OBS	HYCOM	ROMS	
18.5n67.5e	-3.86	-1.93	0.52	0.15	16.86	19.56	18.01	17.8	14.04	251
14.9n69e	-2.92	11.63	0.82	0.72	11.75	18.39	19.6	18.38	9.85	381
12.1n68.6e	-11.22	3.76	0.74	0.94	15	7.64	13.73	13.99	6.91	226
17.8n89.2e	-10.64	10.62	0.9	0.92	14.54	15.6	23.44	21.18	22.09	181
16.3n87.9e	-11.56	11.24	0.86	0.75	16.06	19.43	20.98	17.94	23.06	396
13.5n84.2e	-9.7	5.56	0.63	0.59	18.31	18.17	21.18	12.22	13.12	261
14n87e	-13.75	5.05	0.66	0.85	18.2	9.21	14.8	11.34	11.39	267
6.3n88e	-0.78	21.46	0.84	0.74	16.76	28.74	26.6	18.49	17.05	226

Table 8. D20 statistics of HYCOM and ROMS at RAMA buoy locations

	BIAS (m)		CORR		RMSE (m)		STD (m)			VALID POINTS
Buoy	HYCOM	ROMS	HYCOM	ROMS	HYCOM	ROMS	OBS	HYCOM	ROMS	
12s65e	-1.33	4.73	0.69	0.96	15.09	7.63	20.71	13.84	18.66	294
4s65e	6.25	19.92	0.9	0.75	12.65	25.05	21.71	14.12	12.36	283
5s95e	-1.81	22.28	0.93	0.8	4.9	23.59	12.09	11.85	7.17	151
8s65e	10.14	14.16	0.9	0.9	20.09	20.49	32.55	19.15	26.53	288

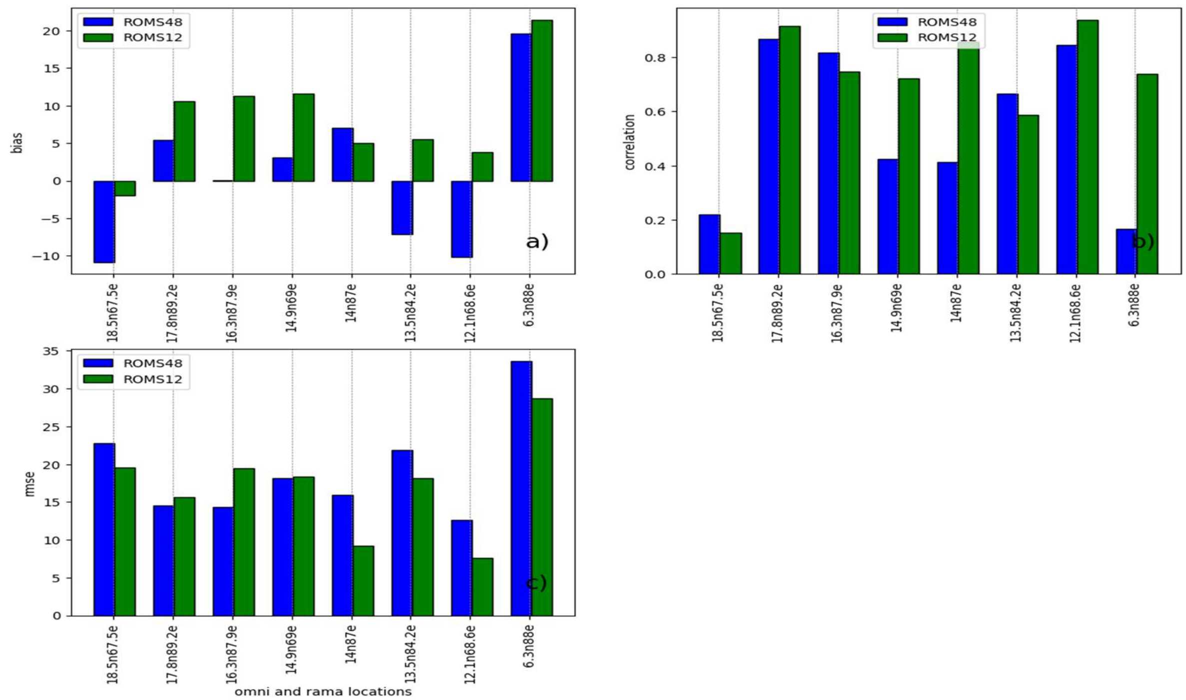

*Figure 38: Location-wise statistics plots of ROMS 1/12 and ROMS 1/48 D20 with respect to OMNI and RAMA buoy observations (a)bias (*m *), (b) correlation coefficient, and (c) RMSE (*m*).*

Basin-scale spatial comparison of MLD from ROMS 1/12 and HYCOM is shown in Figure 39. Although both ROMS and HYCOM are able to capture the observed spatial distribution pattern, ROMS shows much deeper (shallower) MLD over the Arabian Sea (Bay of Bengal). HYCOM MLD spatial distribution pattern shows a closer match with observations as compared to ROMS.

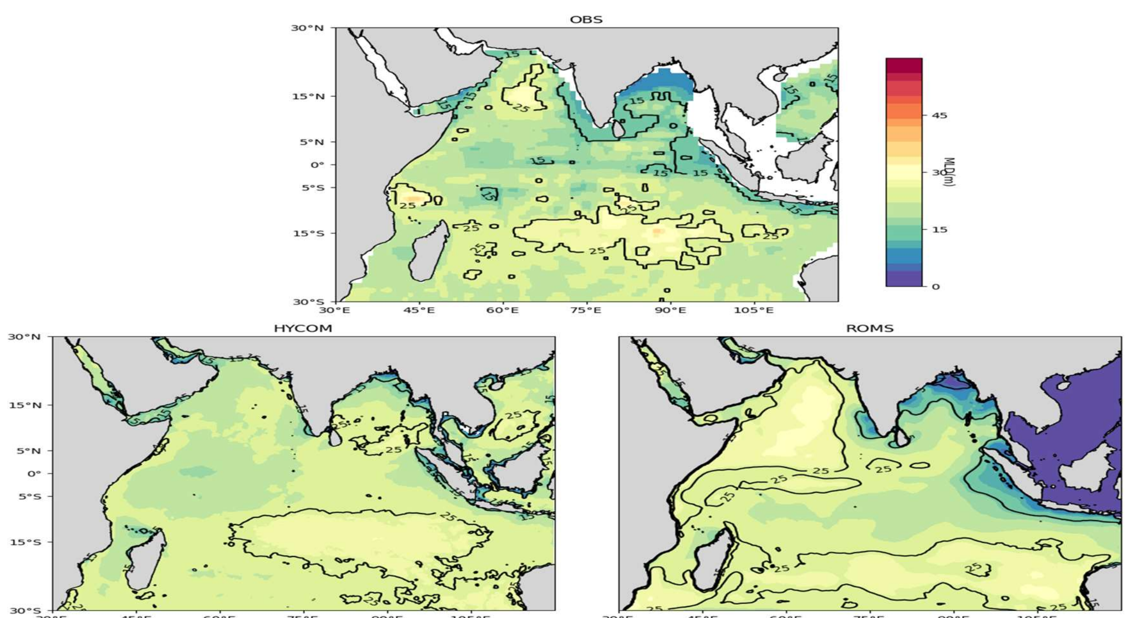

Figure 39: Annual mean spatial MLD (m) from Argo observations (upper panel), HYCOM (lower left panel), and ROMS 1/12 (lower right panel).

The comparison over eastern AS and BoB is shown in Figure 40 for more clarity which also shows model resolution's impact. This figure shows similar results to that of basin scale, but MLD in ROMS 1/12 over the north BoB much improved in ROMS 1/48. This can be seen in the difference plot as well (Figure 41).

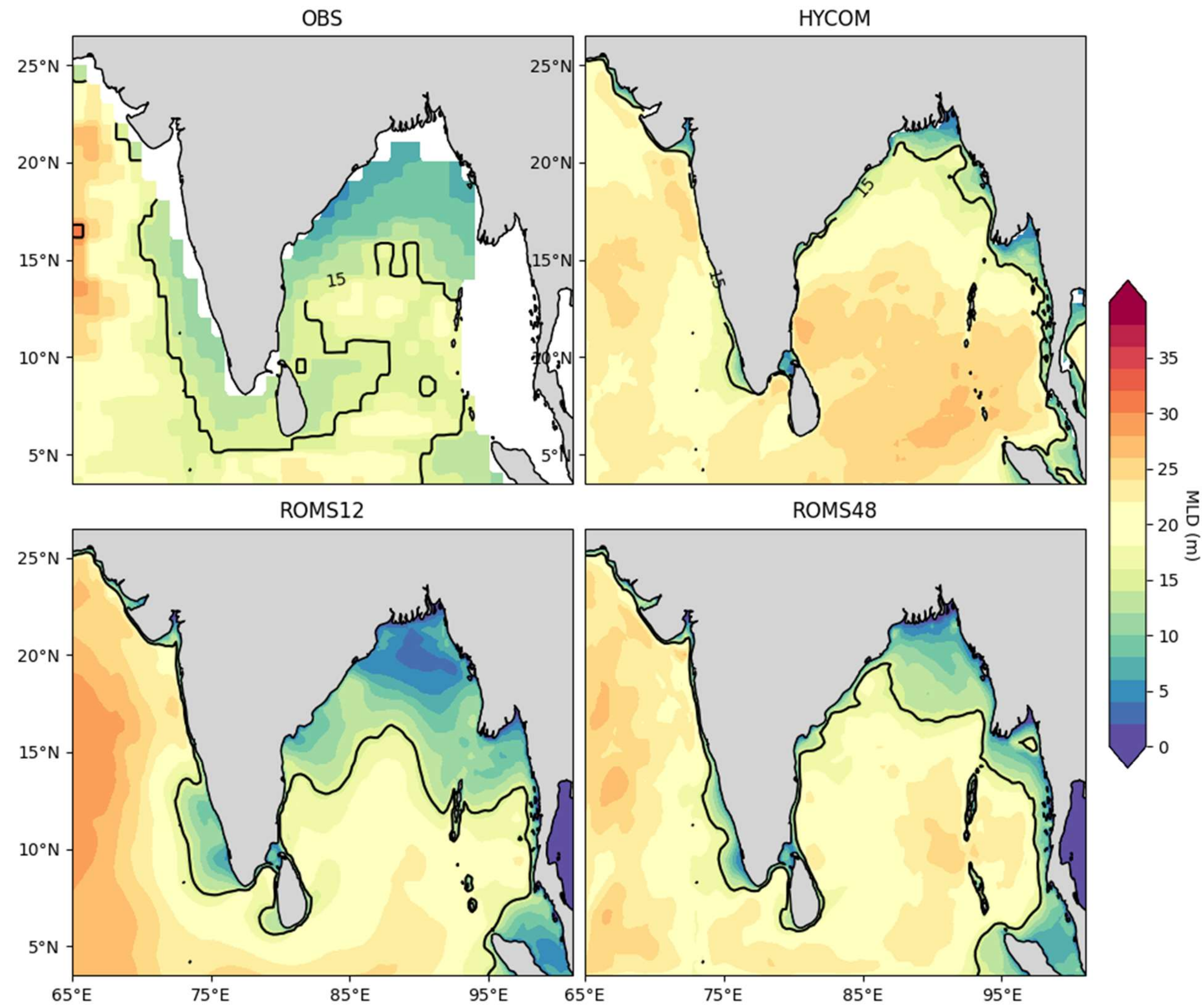

Figure 40: Same as Figure 39 but over the Bay of Bengal which also includes ROMS 1/48.

The seasonal cycle of MLD comparison over different regions is shown in Figure 42. HYCOM performs better than ROMS in all regions except in the eastern equatorial Indian Ocean where ROMS performance is better than HYCOM. Over the western equatorial and thermocline ridge region HYCOM remarkably reproduces the seasonal cycle. The observed bi-modal seasonal variation over the AS is also better captured in HYCOM as compared to ROMS. The statistical comparison of these regions is given in Table 9.

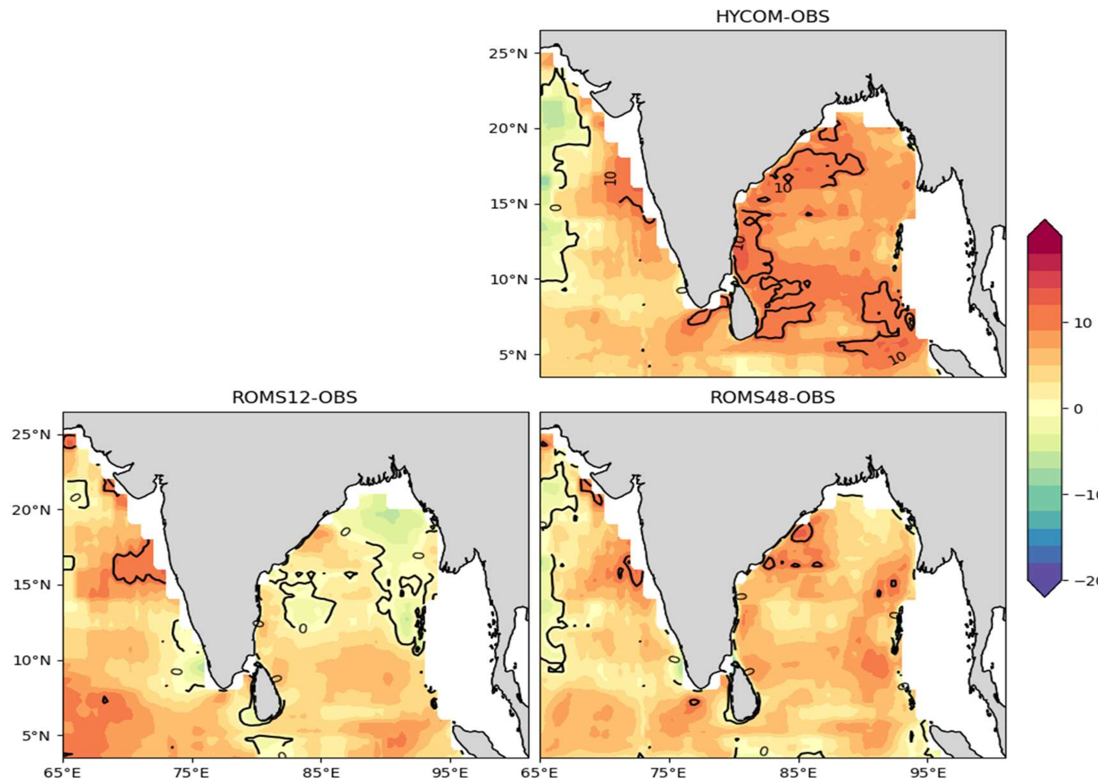

Figure 41: Annual mean spatial bias of MLD (m) over the BoB with respect to Argo observations.

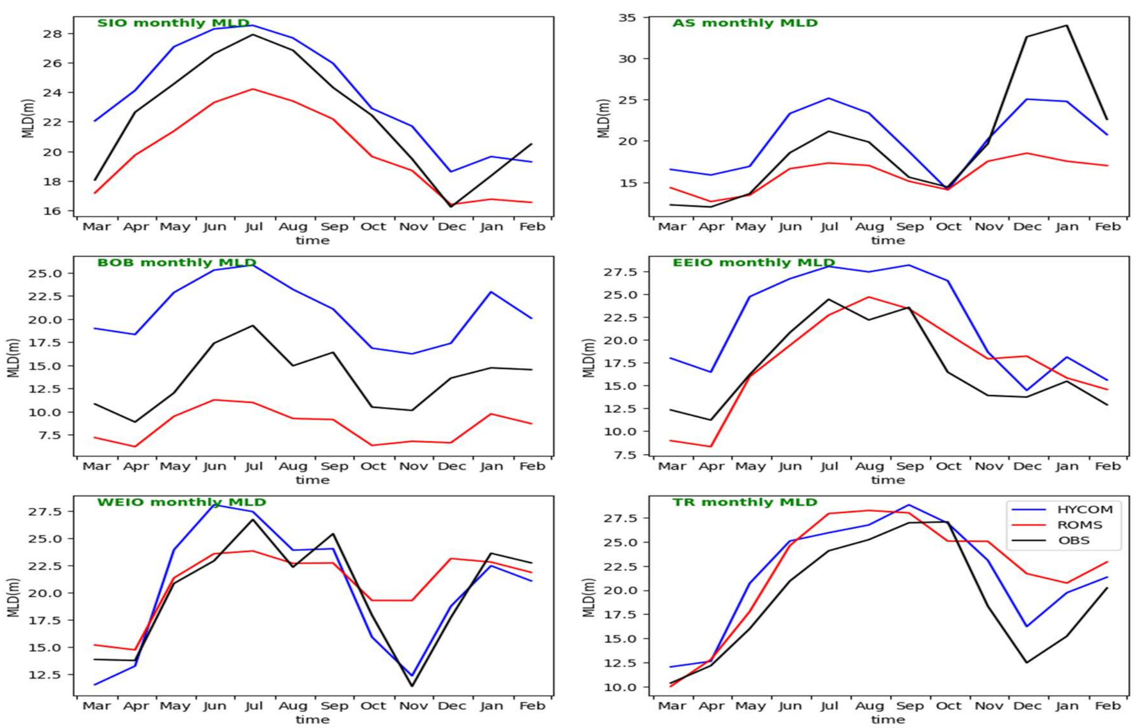

Figure 42: MLD (m) seasonal cycle of Argo observations, HYCOM, and ROMS 1/12 averaged over the different regions defined in Figure 1b.

9. Region-wise MLD statistics with monthly RG-Climatology

Regions as defined in Figure 1b	BIAS (m)		CORR		RMSE (m)		STD (m)		
	HYCOM	ROMS	HYCOM	ROMS	HYCOM	ROMS	OBS	HYCOM	ROMS
SIO	1.5	-2.38	0.94	0.96	1.94	2.69	3.67	3.49	2.78
AS	0.7	-3.76	0.8	0.83	4.57	6.69	6.95	3.78	1.83
BOB	7.17	-5.13	0.8	0.86	7.42	5.44	3.07	3.14	1.72
EEIO	4.97	0.62	0.89	0.85	5.53	2.71	4.43	5.2	4.99
WEIO	0.29	0.94	0.92	0.8	2.18	3.09	4.76	5.55	3.01
TR	2.51	2.98	0.96	0.86	3.02	4.21	5.65	5.35	5.64

6. Summary and Conclusions

Indian National Centre for Ocean Information Services (INCOIS), Ministry of Earth Science, Government of India mandated to provide the ocean state forecast advisory to the north Indian Ocean including the coast of India. It is also mandated to provide the forecast and advisory to the Indian Ocean RIMES countries. INCOIS operationalized ¼ degree ROMS in 2010 to provide a 5-7-day forecast of ocean circulation over the Indian Ocean. Subsequently, it was upgraded to 1/12 degrees in 2016. Further 1/16-degree HYCOM was operationalized in 2018. ROMS forecast was generated using atmospheric forcing from the National Canter for Medium-Range Weather Forecast (NCMRWF). However, HYCOM uses GFS forcing. In this report, we evaluated the first-day surface and sub-surface current, sea surface temperature (SST), MLD, and D20 forecast of operational INCOIS OGCMs i,e ROMS, and HYCOM. We used independent data sets from in-situ buoy observations as well as satellite observations to see the mean, bias, correlation coefficients (CC) RMSE, and skill score (SS). Overall, ROMS 1/12 shows marginally better performance against the observations relative to HYCOM in terms of statistical performance for SST and surface current. However, for sub-surface current, MLD and D20 HYCOM perform better than ROMS 1/12. Although there are significant differences in the configurations both models are shown to be statistically equivalent with consistent spatial and temporal patterns indicating the main differences are attributable to unrepresented processes. Overall ROMS 1/12 performance is slightly better than HYCOM in SST. Allan Murphy, a pioneer in the field of forecast verification, wrote an essay on what makes a forecast "good" (Murphy,1993). A skill *score* measures the *accuracy* of a forecast with reference to the accuracy of a *standard forecast*. The standard forecast is generally considered from a long-term climatology. We used Morphy's 1993 methods to compute skill scores. We used in-situ buoy observed SST and current for the evaluation of the ROMS 1/12 and HYCOM forecasted fields. Since the buoy observations are available for a shorter duration and also suffer data gaps, the climatology computed from these in-situ observations may not be true representative. Hence, using this climatology as a reference forecast for SS computation may give unrealistic values. Therefore we used long-term daily NOAA-OI SST observation (1982-2020) and daily current speed from OSCAR (1992-2022) analysis as a reference forecast at the respective buoy locations for SS computation. The ROMS 1/12 SS values for SST forecast ranged from 0.2-0.8 whereas for HYCOM these values are 0.2-0.5 with respect to OMNI buoy observations. When repeating this with 14 RAMA buoys similar results were reflected. But at 8 °S and 80.5 °E ROMS SS values show negative which also falls over the EEIO where ROMS SS values also show negative. Hence, it can be concluded over the EEIO 1st days SST forecast shows poor skill for ROMS. However, for SST skill score HYCOM performs better in the eastern equatorial Indian Ocean.

For the surface current forecast, ROMS1/12 performs slightly better than HYCOM in terms of bias, CC, STD, and RMSE. We used OMNI and RAMA buoy observed current to evaluate the first-day forecasted current for ROMS1/12 and HYCOM. We used the entire duration of the available buoy observations (2012-2022) to compute surface current speed climatology for the reference forecast in the Murphys skill score computation. However, due to a lot of data gaps and also for shorter periods of data availability, the daily climatology made at OMNI and RAMA buoy locations may not be robust. Based on this daily climatology as a reference forecast current skill shows negative in almost all the locations. Hence, we further used STD from buoy as a reference and also daily OSCAR climatology made from 1992-2022. Skill Score computed based on STD shows negative values like buoy climatology as a reference implies poor skill. However, based on OSCAR climatology as a reference forecast, SS shows positive in all OMNI and RAMA buoy locations. It is to be noted that in 2020, during the study year, there were a lot of data gaps in, many buoy locations. Hence, we choose to use those buoys where at least 200 days of observations are available for both SST and surface current. Subsurface current speeds at 25 m, 50, and 100 m depths of HYCOM and ROMS are unable to capture the buoy observed current speed at all these three depths. HYCOM performed slightly better as compared to ROMS in terms of daily variability. Both HYCOM and ROMS 1/12 are unable to capture the EICC structure and speed. ROMS 1/12 current speed over the EICC region is very much underestimated as compared to HF radar observations, with HYCOM performing slightly better. Most of the eddies in the western Bay of Bengal (BoB) are unable to be captured by ROMS 1/12 despite its eddy-resolving model. ROMS 1/48 shows the presence of spurious eddies which are not seen in OSCAR analysis. On the other hand, HYCOM can capture the location as well as the magnitude of the eddies seen in sea level anomaly plots from altimeter observations. We further show that enhanced resolution of ROMS from 1/12 degrees to 1/48 degrees degraded the skill of current and SST forecast when evaluated with the in-situ and satellite observations. However, near the coast, the RMSE errors were reduced in 1/48 as compared to 1/12-degree ROMS for SST. Both HYCOM and ROMS 1/12 show basin scale deeper D20 when compared with Argo observations as well as buoy observations except BoB where HYCOM shows shallower D20. The seasonal cycle of observed D20 over the western and eastern equatorial Indian Ocean is remarkably reproduced in HYCOM. Similar results were also found for the MLD. However, in the case of MLD ROMS 1/12 seasonal cycle is better reproduced over the eastern equatorial Indian Ocean as compared to HYCOM. HYCOM(ROMS 1/12) shows deeper (shallower) MLD over the BoB. Like SST and current for D20 and MLD too enhanced spatial resolution in ROMS from 1/12 to 1/48 degree, degrades the forecast as compared to 1/12 degree resolution. This study further confirms the finding of Hyder et al. (2012) which shows no skill enhancement on hindcast surface current in the high resolution (1/12°) regional model compared to the coarser resolution (1/4°) global model over the Indian Ocean

References:

Anderson J.L. Exploring the need for localization in ensemble data assimilation using a hierarchical ensemble filter Physica D, 230 (2007), pp. 99-111, 10.1016/j.physd.2006.02.011

Arunraj, K. S., Jena, B. K., Suseentharan, V., & Rajkumar, J. (2018). Variability in Eddy distribution associated with east India coastal current from high-frequency radar observations along southeast coast of India. Journal of Geophysical Research: Oceans, 123, 2018JC014041. https://doi.org/10.1029/ 2018jc014041

Acharya, R., and S. Chattopadhyay, 2019: OMNI (Ocean Moored buoy network for northern Indian Ocean) Buoy System—a critical component of ocean observational programme of ESSO (earth System Science organization), Ministry of /Earth Sciences, Government of India. *Journal of Indian Geophysical Union*, 23(1), 101-105

Beal, L., and Coauthors, 2020: A Road Map to IndOOS-2: Better Observations of the Rapidly Warming Indian Ocean. *Bulletin of the American Meteorological Society*. 101. E1891–559 E1913. 10.1175/BAMS-D-19-0209.1.

Baduru B., Paul B., Banerjee D.S., Sanikommu S., Paul A. Ensemble based regional ocean data assimilation system for the Indian ocean: Implementation and evaluation Ocean Model., 143 (2019) https://doi.org/10.1016/j.ocemod.2019.101470

Blockley, E.W., Martin, M.J., Hyder, P., 2012. Validation of FOAM near-surface ocean current forecasts using Lagrangian drifting buoys. Ocean Sci. 8, 551–565. http: //dx.doi.org/10.5194/os-8-551-2012.

Bonjean, F., and G. S. E. Lagerloef, (2002). Diagnostic model and analysis of the surface currents in the tropical Pacific Ocean. *J. Phys. Oceanogr*., vol. 32, pg. 2938-2954.

Deser, C., M. A. Alexander, and M. S. Timlin (2003), Understanding the persistence of sea surface temperature anomalies in midlatitudes, *J. Clim.*, **16**, 57–72.

Francis, P. A., Vinayachandran,P. N., and Shenoi,S. S. C., 2013: The Indian Ocean Forecast System. *Curr. Sci.*, 104, 1354–1368, www.currentscience.ac.in/Volumes/104/10/1354.pdf.

Francis, P. A., and Coauthors, 2020: High-Resolution Operational Ocean Forecast and Reanalysis System for the Indian Ocean. Bull. Amer. Meteor. Soc., 101, E1340–E1356, https://doi.org/10.1175/BAMS-D-19-0083.1.

George, J P., S. Indira Rani, Jayakumar, A. , Mohandas,S., Mallick,S., Lodh,A., Rakhi,R., Sreevathsa M. N. R., and Rajagopal E. N., (2016): NCUM Data Assimilation System, NMRF/TR/01/2016, 20p

Hyder, P., Storkey,D., Blockley,E., Guiavarc'h,C., Siddorn,J., Martin, M., and Lea, D., (2012) Assessing equatorial surface currents in the FOAM Global and Indian Ocean models against observations from the global tropical moored buoy array, Journal of Operational Oceanography, 5:2, 25-39, DOI: 10.1080/1755876X.2012.11020136

Hunt B.R., Kostelich E.J., Szunyogh I. (2007) Efficient data assimilation for spatiotemporal chaos: A local ensemble transform kalman filter
Physica D, 230 , pp. 112-126, 10.1016/j.physd.2006.11.008

Helber, R. W., Barron, C. N. , Carnes,M. R., and Zingarelli, R. A., (2008), Evaluating the sonic layer depth relative to the mixed layer depth, J. Geophys. Res., 113, C07033, doi:10.1029/2007JC004595.

Joseph,S., Srinivasu,U., Vijay,P., Srinivasan,A., Siva Reddy, S.,(2018) A Report on implementation of operational Global and Indian Ocean HYCOM at INCOIS
INCOIS Technical Report 2018 ESSO-INCOIS-CSG-TR-01-2018

Kara, A. B., and H. E. Hurlburt (2006), Daily inter-annual simulations of SST and MLD using atmospherically forced OGCMs: Model evaluation in comparison to buoy time series, *J. Mar. Syst.*, **62**, 95–119.

Mao, Q., S. W. Chang, and R. L. Pfeffer (2000), Influence of large-scale initial oceanic mixed layer depth on tropical cyclones, *Mon. Weather Rev.*, **128**, 4058–4070.

McPhaden, M. J., and Coauthors, 2009: RAMA: The Research Moored Array for African– Asian–Australian Monsoon Analysis and Prediction. *Bull. Amer. Meteor. Soc.*, 90, 459–598 480, https://doi.org/10.1175/2008BAMS2608.1.

Monterey, G., and S. Levitus, (1997) Seasonal Variability of Mixed Layer Depth for the World Ocean, NOAA Atlas NESDIS, vol. 14, 100 pp., Natl. Oceanic and Atmos. Admin., Silver Spring, Md., 1997.

Murphy, A. H., 1993: What Is a Good Forecast? An Essay on the Nature of Goodness in Weather Forecasting. Wea. Forecasting, 8, 281–293, https://doi.org/10.1175/1520-0434(1993)008<0281:WIAGFA>2.0.CO;2.

Ott E., Hunt ,B.R., Szunyogh, I., Zimin, A.V., Kostelich, E.J., Corazza, M., Kalnay, E., Patil, D.J., Yorke, J.A. (2004)A local ensemble kalman filter for atmospheric data assimilation Tellus A , 10.1111/j.1600-0870.2004.00076.x

Prakash, S., Prakash, P., and Ravichandran, M., (2013) Can oxycline depth be estimated using sea level anomaly (SLA) in the northern Indian Ocean?, Remote Sensing Letters, 4:11, 1097-1106, DOI: 10.1080/2150704X.2013.842284

Reynolds, R. W., Smith,T. M., Liu,C., Chelton,D. B., Casey,K. S., and Schlax,M. G., (2007)Daily high-resolution-blended analyses for sea surface temperature. *Journal of Climate*, 20, 5473–5496, doi:10.1175/JCLI-D-14-00293.1

Ravichandran,M., Behringer, D., Sivareddy, S.,Girishkumar, M.S., Chacko, N., Harikumar, R. (2013) Evaluation of the global ocean data assimilation system at INCOIS: the tropical Indian Ocean. Ocean Modelling 69:123–135.https://doi.org/10.1016/j.ocemod.2013.05.003

Rahaman, H., Behringer, D.W., Penny, S.G., Ravichandran, M., (2016) Impact of an upgraded model in the NCEP Global Ocean Data Assimilation System: The tropical Indian Ocean. Journal of Geophysical Research: Oceans 121(11):8039-8062.https://doi.org/10.1002/2016JC012056.

Rahaman, H., Venugopal, T., Penny, S.G., Behringer, D., Ravichandran, M., Raju, J.V.S. et al (2018) Improved Ocean analysis for the Indian Ocean.JournalOfOperational Oceanography 12(1):16-33.https://doi.org/10.1080/1755876X.2018.1547261

Rao, S. A., Goswami, B.N., Sahai, A.K., Rajagopal, E.N., Mukhopadhyay, P., Rajeevan, M., Nayak, S., Rathore, L.S., Shenoi, S.S.C., Ramesh, K.J., Nanjundiah, R.S., Ravichandran, M., Mitra, A.K., Pai, D.S., Bhowmik, S.K.R., Hazra, A., Mahapatra, S., Saha, S.K., Chaudhari, H.S., Joseph, S., Sreenivas, P., Pokhrel, S., Pillai, P.A., Chattopadhyay, R., Deshpande, M., Krishna, R.P.M., Das, R.S., Prasad, V.S., Abhilash, S., Panickal, S., Krishnan, R., Kumar, S., Ramu, D.A., Reddy, S.S., Arora, A., Goswami, T., Rai, A., Srivastava, A., Pradhan, M., Tirkey, S., Ganai, M., Mandal, R., Dey, A., Sarkar, S., Malviya, S., Dhakate, A., Salunke, K., and Maini, P.: Monsoon Mission: A Targeted Activity to Improve Monsoon 535 Prediction across Scales. Bull. Amer. Meteor. Soc., 100, 2509–2532, https://doi.org/10.1175/BAMS-D-17-0330.1, 2019.

Roemmich, D. and J. Gilson, (2009) The 2004-2008 mean and annual cycle of temperature, salinity, and steric height in the global ocean from the Argo Program. *Progress in Oceanography*, **82,** 81-100.

Saima, A., Brassington, G.B., Divakaran, P., Régnier, C., Drévillon, M., Maksymczuk, J., Peterson K. A., Verification and intercomparison of global ocean Eulerian near-surface currents,Ocean Modelling, (2023)Vol 186, ,102241,ISSN 1463-5003, https://doi.org/10.1016/j.ocemod.2023.102241.

Sikhakolli , R. , Sharma , R. , Basu , S. , Gohil , B.S. , Sarkar , A. and Prasad , K.V.S.R. (2012) Evaluation of OSCAR ocean surface current product in the tropical Indian Ocean using in situ data . *Journal of Earth System Science 2013* 122, No. 1, February 2013, pp. 187–199.

Sumit Kumar, A. Jayakumar, M. T. Bushair, Buddhi Prakash J., Gibies George, Abhishek Lodh, S. Indira Rani, Saji Mohandas, John P. George and E. N. Rajagopal (2018). Implementation of New High Resolution NCUM Analysis-Forecast System in Mihir HPCS , NMRF/TR/01/2018.

Siegel, D. A., Doney,S. C., and Yoder, J. A., (2002), The North Atlantic spring phytoplankton bloom and Sverdrup's critical depth hypothesis, *Science*, **296**, 730–733.

Venkatesan, R., Lix, J.K., Phanindra Reddy, A., Arul Muthiah, M. and Atmanand, M.A., (2016a). Two decades of operating the Indian moored bouy network: significance and impact, J. Operational Oceanography, 9, 45-54.

Venkatesan, R., Krishnan,K.P ., Muthiah,M .A., Kesavakumar,B., Divya,D. T., Atmanand,M.A., Rajan, S., and Ravichandran, M. (2016b) Indian moored observatory in the Arctic for long-term in situ data collection.The International Journal of Ocean and Climate Systems 7(2):55-61DOI: 10.1177/1759313116642898

Wang, X., Bishop, C.H.A, (2003) comparison of breeding and ensemble transform Kalman filter ensemble forecast schemes J. Atmos. Sci., 60 , pp. 1140-1158, 10.1175/1520-0469(2003)060¡1140:ACOBAE¿2.0.CO;2

Webb, P.: Introduction to Oceanography, Roger Williams University, http://rwu.pressbooks.pub/webboceanography (last access: May 2024).